

Increased Advanced Glycation Endproducts, Stiffness, and Hardness in Iliac Crest Bone From Postmenopausal Women With Type 2 Diabetes Mellitus on Insulin

Sashank Lekkala, ¹ • Sara E Sacher, ¹ • Erik A Taylor, ² Rebecca M Williams, ³ Kendall F Moseley, ⁴ and Eve Donnelly ^{1,5} •

ABSTRACT

Individuals with type 2 diabetes mellitus (T2DM) have a greater risk of bone fracture compared with those with normal glucose tolerance (NGT). In contrast, individuals with impaired glucose tolerance (IGT) have a lower or similar risk of fracture. Our objective was to understand how progressive glycemic derangement affects advanced glycation endproduct (AGE) content, composition, and mechanical properties of iliac bone from postmenopausal women with NGT (n=35, age $=65\pm7$ years, HbA1c $=5.8\%\pm10^{-2}$ 0.3%), IGT (n=26, age $=64\pm 5$ years, HbA1c $=6.0\%\pm 0.4\%$), and T2DM on insulin (n=25, age $=64\pm 6$ years, $HbA1c = 9.1\% \pm 2.2\%$). AGEs were assessed in all samples using high-performance liquid chromatography to measure pentosidine and in NGT/T2DM samples using multiphoton microscopy to spatially resolve the density of fluorescent AGEs (fAGEs). A subset of samples (n = 14 NGT, n = 14 T2DM) was analyzed with nanoindentation and Raman microscopy. Bone tissue from the T2DM group had greater concentrations of (i) pentosidine versus IGT (cortical +24%, p=0.087; trabecular +35%, p=0.007) and versus NGT (cortical +24%, p=0.087; trabecular +35%, p=0.007) and versus NGT (cortical +24%, p=0.087; trabecular +35%, p=0.007) and versus NGT (cortical +24%, p=0.087; trabecular +35%, p=0.007) and versus NGT (cortical +24%, p=0.087; trabecular +35%, p=0.007) and versus NGT (cortical +24%, p=0.087; trabecular +35%, p=0.007) and versus NGT (cortical +24%, p=0.087; trabecular +35%, p=0.007) and versus NGT (cortical +24%, p=0.087; trabecular +35%, p=0.007) and versus NGT (cortical +24%, p=0.087; trabecular +35%, p=0.007) and versus NGT (cortical +24%, p=0.087; trabecular +35%, p=0.007) and versus NGT (cortical +24%, p=0.087; trabecular +35%, p=0.007) and versus NGT (cortical +24%, p=0.087; trabecular +35%, p=0.007) and versus NGT (cortical +24%, p=0.087; trabecular +35%, p=0.007) and versus NGT (cortical +24%, p=0.087; trabecular +35%, p=0.007) and +35%, +3tical +40%, p = 0.003; trabecular +35%, p = 0.004) and (ii) fAGE cross-link density versus NGT (cortical +71%, p < 0.001; trabecular +44%, p < 0.001). Bone pentosidine content in the IGT group was lower than in the T2DM group and did not differ from the NGT group, indicating that the greater AGE content observed in T2DM occurs with progressive diabetes. Individuals with T2DM on metformin had lower cortical bone pentosidine compared with individuals not on metformin (-35%, p = 0.017). Cortical bone from the T2DM group was stiffer (+9%, p=0.021) and harder (+8%, p=0.039) versus the NGT group. Bone tissue AGEs, which embrittle bone, increased with worsening glycemic control assessed by HbA1c (Pen: $R^2 = 0.28$, p < 0.001; fAGE density: $R^2 = 0.30$, p < 0.001). These relationships suggest a potential mechanism by which bone fragility may increase despite greater tissue stiffness and hardness in individuals with T2DM; our results suggest that it occurs in the transition from IGT to overt T2DM. © 2022 American Society for Bone and Mineral Research (ASBMR).

KEY WORDS: bone; glycation; material properties; prediabetes; type 2 diabetes

Introduction

ndividuals with type 2 diabetes mellitus (T2DM) are at increased risk of bone fracture despite normal to high bone mineral density (BMD) compared with those without diabetes. The increased fracture risk persists even after adjusting for the greater BMD, body mass index (BMI), and risk of falls typically observed in individuals with T2DM. In contrast, individuals with impaired glucose tolerance (IGT), or prediabetes, have a lower or similar risk of fracture compared with individuals

with normal glucose tolerance (NGT).^(8,9) This reduced fracture risk in individuals with IGT may be explained by greater BMD.^(8,10) However, individuals with T2DM also have higher BMD compared with individuals with IGT or NGT⁽⁸⁾ and paradoxically have a greater risk of fracture. This observation suggests that although those with T2DM maintain BMD, the progression from IGT to T2DM may result in deleterious metabolic or biochemical changes that degrade bone tissue properties.⁽¹⁰⁻¹³⁾

T2DM is characterized by peripheral insulin resistance as well as progressive loss of pancreatic β -cell function, resulting in

Received in original form March 17, 2022; revised form November 25, 2022; accepted December 2, 2022.

Address correspondence to: Eve Donnelly, PhD, Department of Materials Science and Engineering, Cornell University, 227 Bard Hall, Ithaca, NY 14853, USA. E-mail: eve.donnelly@cornell.edu; Kendall F Moseley, MD, Division of Endocrinology, Diabetes & Metabolism, Metabolic Bone and Osteoporosis Center, Johns Hopkins University School of Medicine, 5501 Hopkins Bayview Circle, 2A62, Asthma and Allergy Center, Baltimore, MD 21224, USA. E-mail: kmosele4@jhmi.edu Additional Supporting Information may be found in the online version of this article.

Journal of Bone and Mineral Research, Vol. 38, No. 2, February 2023, pp 261–277. DOI: 10.1002/jbmr.4757

 $\ensuremath{\texttt{©}}$ 2022 American Society for Bone and Mineral Research (ASBMR).

¹Department of Materials Science and Engineering, Cornell University, Ithaca, NY, USA

²Sibley School of Mechanical and Aerospace Engineering Cornell University, Ithaca, NY, USA

³Meinig School of Biomedical Engineering Cornell University, Ithaca, NY, USA

⁴Division of Endocrinology, Johns Hopkins University School of Medicine, Baltimore, MD, USA

⁵Research Division, Hospital for Special Surgery, New York, NY, USA

insulin secretion decline over time.⁽¹⁴⁾ Most of the individuals with T2DM will eventually require exogenous insulin, and the odds of insulin therapy requirements increase with T2DM duration.^(15,16) Further, individuals with T2DM on insulin have a higher fracture risk than individuals with T2DM not on insulin,^(4,9,17) making this cohort important to examine. On the other hand, metformin, a diabetic medication, improves bone mass and decreases fracture risk in individuals with T2DM.^(18,19)

The mechanisms responsible for increased fracture risk in individuals with T2DM are not well understood. One hypothesized mechanism by which bone strength, composition, and material properties may be altered in individuals with T2DM involves impaired bone remodeling with subsequent accumulation of advanced glycation endproducts (AGEs).^(11,13) Reduced bone formation in individuals with T2DM was observed in histomorphometric studies^(20,21) and corroborated by lower serum levels of bone formation and resorption markers.^(22,23) Similar trends of bone turnover markers were observed in prediabetic individuals.⁽²⁴⁾

Hyperglycemia in individuals with T2DM can lead to formation of AGEs via nonenzymatic glycation of amino acid residues on collagen. (25-27) These AGEs accumulate in bone with age^(28,29) and embrittle (reduced fracture toughness) the tissue. (25,30) On the other hand, enzymatic cross-links are formed in a controlled manner regulated by lysyl oxidase and increase whole bone strength. (31) Pyridinoline, a mature enzymatic cross-link, was lower in trabecular bone from men with T2DM compared with non-DM men. (25) The mechanism for reduced enzymatic cross-linking and its effect on bone strength in individuals with T2DM is unknown. Impaired osteoblast function in individuals with T2DM, (32) which regulate lysyl oxidase secretion, can lead to reduced enzymatic cross-linking. Additionally, excessive nonenzymatic cross-linking may reduce the bonding sites for the formation of enzymatic cross-links. (33) Therefore, a detrimental combination of increased AGEs, and consequently reduced enzymatic cross-linking, is a potential mechanism for increased fracture risk in individuals with T2DM.

Recent studies of clinical specimens from individuals with T2DM reported differences in bone compositional and material properties. Bone from individuals with T2DM had greater (i) concentrations of total fluorescent AGEs (fAGEs); (26,34,35) (ii) concentrations of the specific cross-linking AGE, pentosidine; (25,27) and (iii) mineral content, all consistent with reduced remodeling. (25,36-38) These compositional changes had both beneficial and detrimental effects on bone mechanical performance. A few studies reported contrasting results such as lower mineral content, (34) similar total fAGE content, (25,26,37) and similar pentosidine content⁽³⁹⁾ in individuals with T2DM versus non-DM controls. Differences in T2DM duration and severity, as well as bone compartment analyzed (cortical versus trabecular) may explain the variability in the observations. Overall, the tissue from the individuals without the protective effect of higher bone volume fraction was more brittle because of greater concentrations of AGEs. (25)

Numerous gaps remain in our understanding of the factors that drive bone fragility with progression from IGT to T2DM. Although there are animal models indicating that total bone fAGE content is increased even in prediabetic mice compared with lean controls, this result has yet to be confirmed in human populations. Further, lower microscale resistance of cortical bone to in vivo impact indentation and ex vivo cyclic reference point indentation were observed in individuals with T2DM. (26,41-43) However, the changes in bone microstructure or composition responsible for these differences are unknown,

and the outcomes require further validation to associate with tissue material properties. Existing studies have focused primarily on subjects with T2DM sufficiently well controlled for elective total hip arthroplasty. (25,26,44) Cohorts with a wide range of disease severity are required to understand the progression of the changes in bone material properties from normal glucose tolerance to overt T2DM.

The goal of our study was to understand how progressive glycemic derangement affects the AGE content, composition, and mechanical properties of bone matrix. We enrolled postmenopausal women with normal glucose tolerance (NGT), impaired glucose tolerance (IGT), and overt T2DM to investigate the relationships between glucose control and bone strength in transiliac crest bone samples. Our approach included (i) measurement of the nanomechanical and compositional properties of cortical and trabecular bone from individuals with and without T2DM using nanoindentation and Raman spectroscopy, (ii) assessment of the spatial distribution of AGEs and collagen organization in the groups using multiphoton microscopy, and (iii) assessment of the quantity of enzymatic and nonenzymatic collagen crosslinks in all the groups using high-performance liquid chromatography (HPLC). We hypothesized that (i) individuals with T2DM have higher bone mineral content, which results in stiffer and harder tissue, and (ii) AGE content is higher in individuals with T2DM.

Materials and Methods

Study cohort

Postmenopausal women were recruited at Johns Hopkins University as described in a previous study. The current study is an opportunistic secondary extension of an ongoing primary study of histomorphometry and morphology in bone biopsies from individuals with varying levels of glycemic derangement. Using the same biopsies originally collected for histomorphometric analysis, we have extended the primary study (not yet published) by performing secondary analyses of infrared microscopic properties in prior work.

The size of the study cohort was calculated based on the primary histomorphometric outcome of interest for the original study for which biopsies were collected: mineral apposition rate. Power calculations were based on two-sided tests with a power of 0.9 and an effect size of 0.42 in unit of standard deviation, which corresponds to a difference of 0.042 $\mu m/d$ (physiologically important), considering p values <0.05 as statistically significant. There were limited data in the literature on the variability in histomorphometry measurements in women with T2DM and no data in IGT. We hypothesized that bone microarchitecture and mineralization would fall between the parameters of NGT and T2DM. In calculating our sample size, we took all the available data at the time into consideration; however, we looked primarily at the data published by Krakauer and colleagues in a cohort with diabetes as well as that in healthy controls. $^{(21,45)}$

Participants were allocated to three groups: (i) NGT (n=35), if blood glucose level after 2 hours, 75-g oral glucose tolerance test (OGTT) was less than 140 mg/dL; (ii) IGT (n=26), if blood glucose level after OGTT was between 140 mg/dL and 199 mg/dL; and (iii) T2DM (n=23), if diagnosed with T2DM and on insulin therapy \pm oral therapy. Women with T2DM but not on insulin therapy were excluded from the T2DM group to capture the effects of severe T2DM on bone. Further, women with type 1 diabetes,

15234861, 2023. 2, Downoladed from https://asbmr.onlinelibiary.viley.com/doi/10.1002/jbmr.4757 by Comell University, Wiley Online Library on [08/02/2023]. See the Terms and Conditions (https://onlinelibrary.wiley.com/terms-and-conditions) on Wiley Online Library for rules of use; OA articles are governed by the applicable Creative Commons Licenson

chronic kidney disease/nephropathy (creatinine clearance <60 mL/min/1.73 m² by Modification of Diet in Renal Disease [MDRD] equation), a history of fragility fracture, osteoporosis on dual-energy X-ray absorptiometry (DXA), and other metabolic bone diseases (Paget's, hyperparathyroidism, vitamin D deficiency) were excluded from this study. No participant had a history of myocardial infarction or stroke in the last 5 years on intake assessment. Women using medications known to affect bone metabolism were also excluded. Our exclusion criteria were designed to isolate the effects of glycemic derangement on bone composition and material properties with major confounders removed.

All participants provided informed consent, and all study procedures were approved by the Johns Hopkins Medicine Institutional Review Board. The participants completed five visits: (i) initial screening to assess medical history, BMD assessment with DXA of the lumbar spine, femoral neck, and hip (Hologic, Bedford, MA, USA) to rule out osteoporosis, and administer OGTT to determine glycemic control in those not on insulin; (ii) secondary screening to obtain blood and urine samples to measure hemoglobin A1c (HbA1c), markers of bone resorption and formation, 25-hydroxy vitamin D, parathyroid hormone (PTH), and a complete metabolic panel (Table 2); (iii) baseline visit to instruct participants how to prepare for bone biopsy and complete demeclocycline labeling; (iv) visit to obtain iliac crest bone sample; and (v) final visit to remove sutures and address follow-up questions. Participants were compensated for each visit. Participants were instructed to take two courses of demeclocycline, each course lasting 3 days with a 12-day gap between the two courses. The biopsy was obtained 5 days after the second course. The demeclocycline labeling protocol followed by transiliac bone biopsy was initiated within 1 month of the participants' screening and baseline visits, DXA scan, and blood and urine testing. Biopsies were stored in ethanol before tissue processing.

Study design

The primary objective of this study is to understand how progressive glycemic derangement affects bone AGE content. Therefore, pentosidine concentration in both cortical and trabecular bone from all the samples from all three groups was characterized using HPLC. In addition to overall tissue AGE content, differences in glycemic control and bone remodeling rate can alter the spatial distribution of AGEs. We hypothesized that AGEs preferentially accumulate in older tissue regions, which is exacerbated by impaired ability to remodel damaged tissue in individuals with T2DM. This preferential distribution of AGEs is a function of circulating glucose levels and is expected to take several years in high-glucose environments to be able to be visualized. Therefore, spatial distributions of fluorescent AGEs were compared only in T2DM and NGT samples using multiphoton microscopy.

The secondary objective of this study is to understand how glycemic derangement affects bone material properties at the nanoscale. The sample size for nanoindentation was determined from an initial power analysis. For the analysis, we used a power of 0.8 with an alpha of 0.05 to detect a 10% difference based on nanoindentation data from studies of clinical bone samples with other mineralization defects (osteogenesis imperfecta and osteoporosis)⁽⁴⁸⁻⁵¹⁾ because no nanoindentation data were available at the time from bone from individuals with T2DM. The lower bone turnover observed in T2DM is expected to allow greater

secondary mineralization of the matrix and result in increased stiffness and hardness of this older tissue. (52-54) Therefore, to identify samples that reflected the greatest effect of decreased turnover on material properties, samples with the lowest CTX were chosen from the NGT and T2DM groups. Because no differences in BMD and bone turnover markers were observed in the IGT versus NGT groups, which may reflect similar extent of secondary mineralization and comparable stiffness, the nanomechanical properties of the IGT group were not characterized. The compositional properties of this cohort were previously published, (38) and the purpose of the Raman spectroscopy was to facilitate spatially resolved correlations of mechanical and compositional properties.

Fluorescence microscopy

Demeclocycline labels were visualized in a dark room using a fluorescence microscope (BX43, Olympus, Tokyo, Japan) with a GFP filter (Ex 482/18, Em 520/28) and two air objectives (20 \times , 0.7NA; 10 \times , 0.4 NA; Olympus). In each sample, three labeled trabeculae that spanned the whole biopsy were identified for further characterization of newly formed bone using nanoindentation and Raman spectroscopy.

Nanoindentation

From an initial power analysis, 14 samples with lowest C-telopeptide (CTX) were chosen from each group (NGT and T2DM) to detect a 10% difference in the modulus. The samples with lowest CTX were chosen to determine the effects of reduced remodeling in individuals with T2DM. The biopsies were dehydrated using organic solvents and embedded in poly methyl methacrylate (PMMA). The embedded samples were cut into two halves parallel to the long axis of the cylindrical biopsy (Fig. 1), and all the experiments were performed on one half of the block. The longitudinal sections were anhydrously polished with a series of abrasive grit papers and alumina slurry to achieve a root mean square (RMS) roughness less than 20 nm, (55) as assessed by atomic force microscopy scans of at least four $5 \times 5 \ \mu m^2$ areas per sample. Specimens were rehydrated in Hank's balanced salt solution (HBSS) for 3 hours before testing. The extent of rehydration was monitored by periodically weighing the samples and confirming that the sample weights reached a plateau. Nanoindentation was performed in 4-hour sessions during which rehydration was maintained (<5% weight loss).

A nanoindenter (Tribolndenter, Hysitron, Bruker, Billerica, MA, USA) with a Berkovich diamond tip was used to collect force versus displacement data. The tip was loaded into the sample at 100 μ N/s, held at the maximum load of 1000 μ N for 30 seconds, and unloaded at 100 μ N/s, which produced indentations with contact depths $\sim\!200$ nm. Indentation modulus and hardness were calculated from the unloading portion of the force-displacement curve as previously described. $^{(55,56)}$

Both cortical and trabecular bone were characterized with nanoindentation. At least 30 indents were made in cortical and trabecular bone to account for the heterogeneity in the tissue. $^{(57,58)}$ In cortical bone, two osteonal and two interstitial regions per sample were characterized. Two osteons were randomly chosen, and 15 equidistant indents were placed across the total width of each osteon. The indentations that fell on PMMA in Haversian canals were excluded. Next, two randomly chosen interstitial regions were characterized with 2 \times 2 grids of indents with 5 μm grid spacing. In trabecular bone, two

trabeculae with fluorescent labels of bone formation (Supplemental Fig. S1) were randomly chosen to study the effect of tissue age on material properties. In each trabecula, three regions were characterized (Fig. 1B). Five indents, spaced 5 µm apart, were made along a line perpendicular to the trabecular edge (i) at the formation label (the "label region"), representing newly formed bone (<24 days old) and (ii) at the opposite trabecular edge without formation labels (the "edge region"), representing bone >24 days old; another five equidistant indents were made along the same line in the center of the trabecula from 30% to 70% the width of trabecula (the "center region") (Fig. 1B).

Raman spectroscopy

Compositional properties of cortical and trabecular bone from the subset of samples that underwent nanoindentation were characterized using Raman spectroscopy. Spectra were acquired using a confocal Raman imaging system (Alpha300R, WITec, Ulm, Germany) with a $\sim\!70$ mW 785 nm laser source focused through

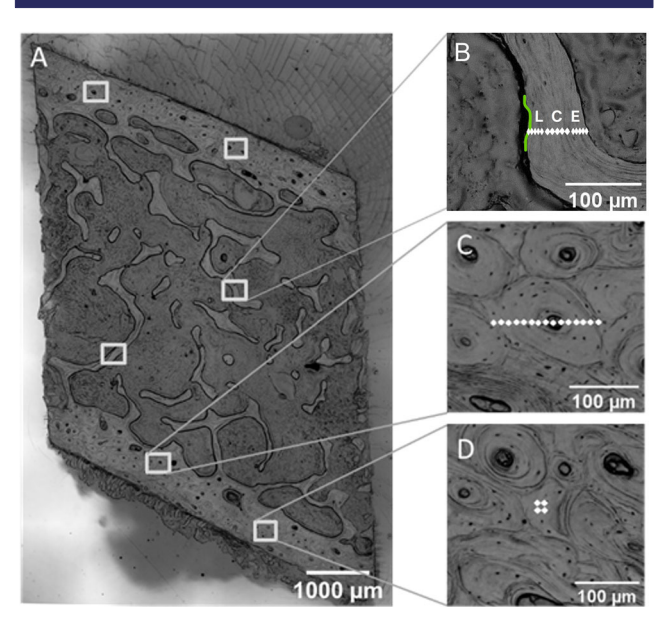


Fig. 1. (A) Stitched optical image of a representative iliac crest biopsy embedded in PMMA. Regions of interest are highlighted with rectangles: (\mathcal{B}) trabecular bone; (\mathcal{C}) osteonal cortical bone; (\mathcal{D}) interstitial cortical bone. Inset images schematically depict locations of indentations: Each rhombus represents an indentation (not to scale). The trabecular regions depict indentations on fluorochrome labels, here indicated by a green line in (\mathcal{B}) and shown in a fluorescence image in Supplemental Fig. S1, in the label (L), center (\mathcal{C}), and opposite edge (E) regions.

a $50\times$, 0.55 NA objective. Each spectrum was averaged from 10 accumulations each obtained with a 6-second integration time.

In cortical bone, at least three osteonal and three interstitial regions were characterized to spatially match the regions characterized by nanoindentation, and the rest of the regions were randomly selected. Three spectra, equidistantly spaced, were collected along a line spanning the radius of each osteon and three spectra spaced 10 μm apart were collected in each interstitial region. In trabecular bone, at least three trabeculae were characterized per sample. Spectra were collected along lines parallel to the surface of each trabecula, at three points spaced 10 μm apart in each of three regions: (i) label: the edge of the trabecula with the bone formation label; (ii) edge: the edge of trabecula without formation label, and (iii) center: the center of the trabecula.

The background fluorescence was subtracted from the spectra using a chemical imaging software (Project FIVE 5.2, WITec, Ulm, Germany). The PMMA contribution to the bone spectra was subtracted. The mineral to matrix ratio (M:M), mineral maturity/ crystallinity (MMC), the carbonate to phosphate ratio (C:P), and glycosaminoglycan (GAG) content (Table 1) were determined by direct integration using a custom code (MATLAB, MathWorks, Natick, MA, USA). The GAG content, which has not yet been extensively validated by gold-standard techniques in bone, is presented in Supplemental Fig. S5. (59,60) Pyridinoline content was calculated by peak fitting the Amide I region using a spectroscopy software (GRAMS/AI, Thermo Fisher Scientific, Pittsburgh, PA, USA). The Amide I region was resolved into four Gaussian sub-bands centered at 1610, 1630, 1660, and 1690. (61)

Confocal/multiphoton microscopy (MPM)

All the samples from the NGT and T2DM groups were imaged with confocal/multiphoton microscopy to collect spatially resolved images of fluorescent AGEs and collagen alignment in cortical and trabecular bone. Three cortical and trabecular regions each $425 \times 425 \ \mu m^2$ previously characterized by nanoindentation and Raman spectroscopy were also characterized with multiphoton microscopy.

The confocal/MPM system (LSM 880, Zeiss, Thornwood, NY, USA) comprises an upright microscope (Axio Examiner.Z1, Zeiss) and multiple laser lines, including the Diode 405-30 unit used for confocal imaging and fully spectrally resolvable emission channels. The system also has a fully integrated Ti:Sapphire (Mai Tai, Spectra Physics, Milpitas, CA, USA) multiphoton excitation source with automated tuning and pulse dispersion control from 700 to 1000 nm. Second harmonic generation (SHG) imaging was performed with a non-descanned filter-based unit. Incident light was focused on the samples using either a $20\times/1.0$ W Plan-Apochromat dipping lens or a $40\times/1.1$ LD C-Aporchromat lens adjusted for a 0.17-mm-thick coverslip on the sample surface.

Table 1. Raman Outcomes and Their Corresponding Peak Area or Intensity Ratio Along With the Integration Ranges

Raman outcome	Peak area or intensity ratio	Integration ranges (cm ⁻¹)	References
Mineral to matrix ratio (M:M)	ν ₂ PO ₄ /Amide III	(410-460)/(1215-1300)	(62)
Mineral maturity/crystallinity (MMC)	1/FWHM of ν_1 PO ₄ (~960 cm ⁻¹)	N/A	(63)
Carbonate to phosphate ratio (C:P)	$\nu_1 \text{ CO}_3/\nu_2 \text{ PO}_4$	(1050-1100)/(410-460)	(64)
Glycosaminoglycan (GAG)	CH₃/Amide III	(1365-1390)/(1215-1300)	(59)
Pyridinoline to amide I ratio (Pyd)	Pyridinoline/Amide I	1660/(1616–1720)	(65)

Abbreviation: FWHM = Full width at half maximum.

 Table 2. Participant Characteristics By Group

Journal of Bone and Mineral Research

Characteristics	NGT	ГОТ	T2DM	NGT versus IGT	NGT versus T2DM	IGT versus T2DM	Chi-square test of independence
n Authorographic	35	26	25				
Antinoponneine Age (years)	64.8 ± 6.8	64.4 ± 5.4	63.8 ± 6.2				
Weight (kg)	76.4 ± 14.6	94.0 ± 22.9	94.3 ± 16.4	p = 0.003	<i>p</i> < 0.001		
Height (cm)	160.8 ± 6.7	$\textbf{165.6} \pm \textbf{6.5}$	160.9 ± 5.9	p = 0.022		p = 0.058	
BMI (kg/m²)	$\textbf{29.6} \pm \textbf{5.6}$	34.3 ± 8.4	36.5 ± 6.9	p = 0.019	p < 0.001		,
Race/ethnicity							χ^2 (6) = 19.883; $p = 0.003$
White, <i>n</i> (%)	27 (77)	13 (50)	6 (24)				
Black, <i>n</i> (%)	8 (23)	11 (42)	17 (68)				
Asian, <i>n</i> (%)	0 (0)	1 (4)	0) 0				
Hispanic, <i>n</i> (%)	0) 0	0 (0)	0) 0				
Other, <i>n</i> (%)	0 (0)	1 (4)	2 (8)				
Bone densitometry, DXA							
Lumbar spine (g/cm^2)	$\textbf{1.18} \pm \textbf{0.17}$	$\textbf{1.28} \pm \textbf{0.23}$	$\textbf{1.28} \pm \textbf{0.19}$				
Total hip (g/cm²)	0.99 ± 0.13	$\textbf{1.03} \pm \textbf{0.13}$	1.09 ± 0.14		p = 0.021		
Femoral neck (g/cm²)	0.93 ± 0.10	$\textbf{0.94} \pm \textbf{0.12}$	1.00 ± 0.14				
T2DM status at baseline visit							
T2DM dx duration (years)	n/a	n/a	14.5 ± 8.4	n/a	n/a	n/a	
OGTT (mg/dL)	95.5 ± 18.2	163.5 ± 29.8	n/a	<0.001	n/a	n/a	
HbA1c (%)	5.8 ± 0.3	6.0 ± 0.4	9.1 ± 2.2		p = 0.008	<0.001	
T2DM-related drugs							
Insulin, <i>n</i> (%)	0) 0	0 (0)	25 (100)				χ 2 (2) = 86; p < < 0.001
Insulin duration (years)	0 + 0	0 ∓ 0	9.3 ± 8.4				
Metformin, n (%)	0 (0)	0)0	14 (56)				χ 2 (2) = 40.802; p < < 0.001
Sulfonylurea, <i>n</i> (%)	(0) 0	0)0	2 (8)				
Other supplements							
Calcium, <i>n</i> (%)	8 (23)	6 (23)	3 (12)				
Vitamin D, <i>n</i> (%)	13 (37)	11 (42)	11 (44)				
Multivitamin, n (%)	15 (43)	10 (38)	4 (16)				
Statin, <i>n</i> (%)	8 (23)	9 (35)	12 (48)				
Acetylsalicylic acid (aspirin), n (%)	15 (43)	7 (27)	12 (48)				
Serum and urinary parameters							
25-hydroxyvitamin D (ng/mL)	33.46 ± 9.41	$\textbf{33.23} \pm \textbf{10.11}$	30.64 ± 7.31				
Creatinine (mg/dL)	0.81 ± 0.16	$\textbf{0.87} \pm \textbf{0.20}$	$\textbf{0.84} \pm \textbf{0.16}$				
Calcium (mg/dL)	9.44 ± 0.30	9.51 ± 0.42	9.44 ± 0.39				
Phosphorous (mg/dL)	3.65 ± 0.49	3.48 ± 0.51	3.57 ± 0.66				
Alkaline phosphatase (U/L)	73.57 ± 17.95	72.96 ± 19.84	88.08 ± 24.09		p = 0.041	p = 0.055	
Parathyroid hormone (pg/mL)	28.77 ± 13.00	39.93 ± 17.59	33.48 ± 16.66	p = 0.028			
eGFR (mL/min/1.73 m²)	80.49 ± 16.29	80.81 ± 13.46	80.08 ± 15.99				
P1NP (ng/mL)	58.78 ± 23.65	57.83 ± 18.62	44.20 ± 14.07		p = 0.014	p = 0.013	
							(Continues)

15234681, 2023, 2, Downloaded from https://asbmr.onlinelibrary.wiley.com/doi/10.1002/jbmr.4757 by Comell University, Wiley Online Library on [08/02/2023]. See the Terms and Conditions (https://onlinelibrary.wiley.com/ and-conditions) on Wiley Online Library for rules of use; OA articles are governed by the applicable Creative Commons License

ENDPRODUCTS 265

Table 2. Continued							
Characteristics	NGT	IGT	T2DM	NGT versus IGT	NGT versus IGT versus T2DM T2DM	IGT versus T2DM	Chi-square test of independence
CTX (ng/mL)	$\textbf{0.32} \pm \textbf{0.18}$	$\textbf{0.31} \pm \textbf{0.22}$	$\textbf{0.22} \pm \textbf{0.11}$		p = 0.043		
Sclerostin (pmol/L)	238.34 ± 98.96	224.50 ± 68.44	229.95 ± 101.36				
ucOC (ng/mL)	3.53 ± 2.00	$\boldsymbol{3.15 \pm 2.13}$	2.66 ± 2.37		p = 0.027		
Pentosidine (nmol/L)	56.25 ± 15.94	51.49 ± 13.54	53.89 ± 13.80				

Note: Values shown are mean \pm standard deviation unless otherwise noted. Statistical significance determined by Kruskal–Wallis H test or chi-square test at a significance level of 0.05.

Abbreviations: NGT = normal glucose tolerance group; IGT = impaired glucose tolerance group; T2DM = type 2 diabetes mellitus group; OGTT = oral glucose tolerance test; eGFR = estimated gloonerular *Note:* Adapted from Hunt et al.⁽³⁸⁾

Itration rate; CTX = carboxy-terminal telopeptide of type 1 collagen; P1NP = amino-terminal propeptide of type 1 collagen; ucOC = undercarboxylated osteocalcin; n/a = not applicable.

Autofluorescence was collected over the range 420 to 485 nm. HBSS was used as the immersion medium for both lenses. To account for different objectives, the power of the incident lasers was scaled to maintain similar fluorescence and SHG intensities at the specimen surface. (66) Otherwise, the power and all settings were kept the same between samples.

To semiquantitatively assess fAGE "cross-link density" (67) for each image, the mean two-photon fluorescence intensity, which reflects the quantity of fluorescent AGEs in the tissue, (68) was normalized to the square root of mean SHG intensity, which reflects the concentration of aligned collagen molecules. (66) This metric is analogous to the total fAGE content measured by fluorometric assay in which the endogenous fluorescence of bone hydrolysate is normalized to the collagen content determined from a colorimetric assay. (25,26) In addition, this method offers key advantages over the fluorometric assay because it is nondestructive and allows for spatially resolved characterization of AGEs.

Confocal imaging was used to obtain semiquantitative spatial distributions of AGE content in cortical and trabecular bone. Images of fluorescent AGEs were obtained by focusing the 405 nm laser on the sample and collecting fluorescence over 430 to 450 nm. $^{(68)}$ In each region, fluorescence was collected from one 1- μ m-thick optical section by adjusting the pinhole aperture to minimize photobleaching.

The endogenous fluorescence from the bone was normalized to that of cascade blue dye (Cascade Blue hydrazide, Trisodium Salt [C-687], Thermo Fisher Scientific), which has a similar excitation-emission profile to AGEs in collagen. The fluorescence intensities of serially diluted calibration standards of 100 μ M C-687 dye in deionized water were measured with the same system settings used to obtain fAGE images. The fluorescence intensity at each pixel was converted to fAGE concentration using calibration curves made from the standards. The mean and the standard deviation of the distribution of normalized fluorescence pixel intensities were calculated for each image.

Collagen organization was assessed from SHG images collected from the same regions. Second harmonic was generated using a circularly polarized laser providing <100 fs pulses at 80 MHz tuned to a wavelength of 780 nm. The incident laser was circularly polarized at the sample using a Berek variable waveplate (5540, New Focus, Irvine, CA, USA) before the scanning box, enabling generation of second harmonic from collagen in all orientations. First-order (mean, standard deviation) and second-order (Supplemental Table S1) statistical parameters of collagen organization were calculated from the images.⁽⁷⁰⁾

High-performance liquid chromatography

HPLC was used to determine the quantity of AGE pentosidine and mature enzymatic cross-links, pyridinoline (Pyd) and deoxypyridinoline (Dpd). All the samples in NGT, IGT, and T2DM were characterized using HPLC. Five samples (2 NGT trabecular, 1 NGT cortical, 1 IGT trabecular, 1 IGT cortical) were excluded because of dilution error in the hydroxyproline assay. The biopsies were de-embedded from PMMA by agitating in methyl acetate (4 days, new solution every 24 hours) and 100% acetone (24 hours). After de-embedding, the biopsies were washed in 100% ethanol (24 hours) and de-fatted in isopropyl ether (15 min \times 3). The tissues were sectioned into cortical and trabecular compartments for separate analysis of each compartment. The separated tissues were rinsed in deionized water, frozen, and lyophilized. The tissues were weighed and hydrolyzed in 1:10 6 N HCl at 110°C for 20 hours. Hydrolysates equivalent to 5 mg of dry bone were dried in a vacuum centrifuge (Savant SPD131DDA

SpeedVac Concentrator, Thermo Fisher Scientific) connected to a refrigerated vapor trap (RVT5105, Thermo Fisher Scientific). Dried powders were resuspended in an internal standard solution (10 nM pyridoxine and 2.4 μ M homoarginine) and filtered with 0.45 μ m syringe filter. The filtered solutions were diluted 1:5 with 10% acetonitrile (v/v) and 0.5% heptafluorobutyric acid (v/v).

The cross-links were separated using two isocratic steps $^{(71)}$ by injecting the diluted solution into a C18 column (3 mm \times 50 mm) (XBridge, Waters Corporation, Milford, MA, USA) integrated in a programmable HPLC system (Alliance e2695, Waters Corporation) attached to a UV–Vis detector (e2475, Waters Corporation). A linear calibration curve was obtained for each HPLC run using serially diluted calibration standard containing pentosidine (Case Western Reserve University), Pyd, and Dpd (8004, Quidel, San Diego, CA, USA).

The cross-link concentrations were normalized by collagen concentrations determined by hydroxyproline concentration from amino acid analysis. For this analysis, the diluted sample from cross-link analysis was further diluted 1:50 with 6 mM homoarginine in 0.1 M borate buffer (pH 11.4). For improved detection, this solution was derivatized using 6 mM fluorenylmethyloxycarbonyl chloride for 40 minutes, and excess reagents and byproducts were extracted three times using pentane. After derivatization, the samples were diluted using 25% (v/v) acetonitrile in 0.25 M boric acid (pH 5.5). The amino acids were separated using the same column and system. (72) A linear calibration curve was obtained for each amino acid run using serially diluted calibration standard containing purified hydroxyproline (Sigma-Aldrich, St. Louis, MO, USA) and 6 μ M homoarginine in 0.1 M borate buffer (pH 11.4).

Statistical analysis

All statistical analyses were performed using a commercial software (JMP Pro 14, SAS Institute, Inc, Cary, NC, USA). All the outcomes were tested for normality using Shapiro-Wilk tests. Log transformation was performed if the data were not normally distributed. Linear mixed effects models were used to assess the effects of study group and tissue region on the characterization outcomes in cortical and trabecular bone separately. The fixed effects were the study group (NGT, IGT, T2DM), tissue region (cortical bone: osteonal, interstitial; trabecular bone: label, edge, center), and the interaction between study group and tissue region. The random effects were the patient ID and the region of interest (two or three regions depending on the method) to account for repeated measures and non-independence in the data. The p values for pairwise comparisons were obtained from Tukey's HSD test. Standard least squares regression modeling was performed to understand the effect of composition on mechanical properties. Significance was set as p < 0.05 for all the outcomes. Data are presented as estimated mean \pm standard deviation or as box and whisker plots on which the p values are the adjusted values from the Tukey HSD tests. The whiskers extend 1.5 times the interquartile range (IQR) from the top and bottom of the box. All the data points including outliers (values greater/less than 1.5 \times IQR) were considered for statistical analysis.

Results

Participant characteristics

Participant characteristics, reported previously for this cohort, (38) are summarized in Table 2. Average age was not different among the groups. Body mass index (BMI) in individuals with IGT and

T2DM was greater compared with individuals with NGT (\pm 16% versus IGT, p=0.019; \pm 23% versus T2DM, p<0.001) but did not differ among IGT and T2DM groups. Average value of glycated hemoglobin (HbA1c) in individuals with T2DM (\pm 2.2%) was greater than in individuals with NGT (\pm 5.8% \pm 0.3%) and IGT (\pm 6.0% \pm 0.4%) (\pm 59% versus NGT, \pm 0.008; \pm 51%

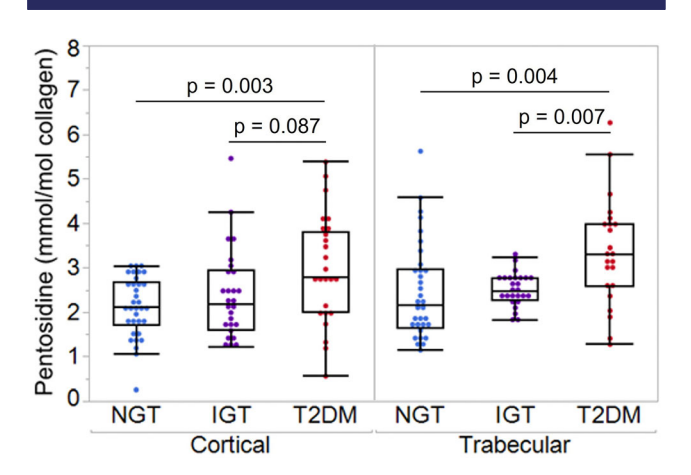


Fig. 2. Box plots of the AGE pentosidine in cortical and trabecular bone. Each overlaid jittered point represents measured (raw) pentosidine concentration in cortical or trabecular bone per specimen. The p values are obtained from linear mixed models adjusted by Tukey's HSD. NGT = normal glucose tolerance; IGT = impaired glucose tolerance; T2DM = type 2 diabetes mellitus.

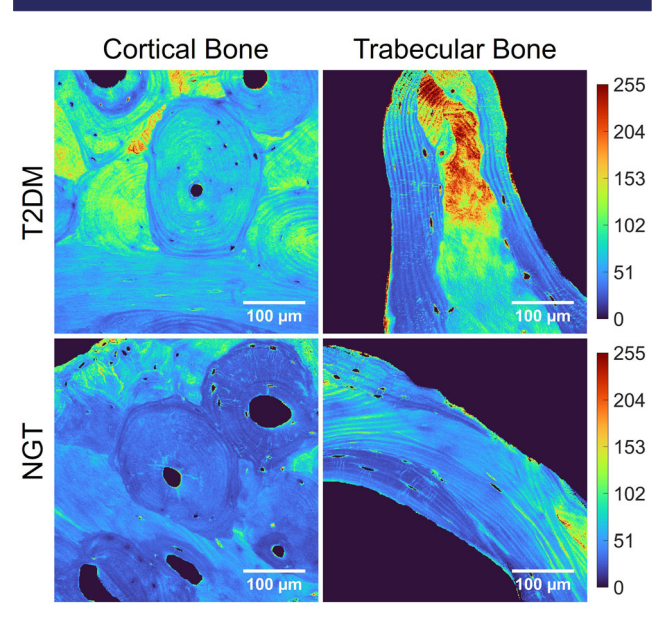


Fig. 3. Representative false color images of fAGE cross-link density in cortical and trabecular bone from NGT (left) and T2DM (right) groups. Color image scale represents fAGE cross-link density calculated as mean two-photon fluorescence intensity normalized to the square root of mean SHG intensity. Scale bar = $100 \ \mu m$. fAGEs = fluorescent advanced glycation endproducts; NGT = normal glucose tolerance; T2DM = type 2 diabetes mellitus.

versus IGT, p < 0.001) but did not differ between IGT and NGT groups. The duration of diabetes was not statistically different among patients who took metformin (16 years) and the patients who did not (12 years). BMD at the lumbar spine and the femoral neck did not differ across the groups. BMD of the total hip was higher in individuals with T2DM compared with individuals with NGT (+9% versus NGT, p = 0.021) but did not differ between IGT and T2DM groups.

The markers of bone turnover were lower in individuals with T2DM compared with individuals with NGT. In the T2DM group, N-terminal propeptide of type 1 collagen (P1NP), a marker of bone formation, was 25% lower (p=0.013) and C-terminal

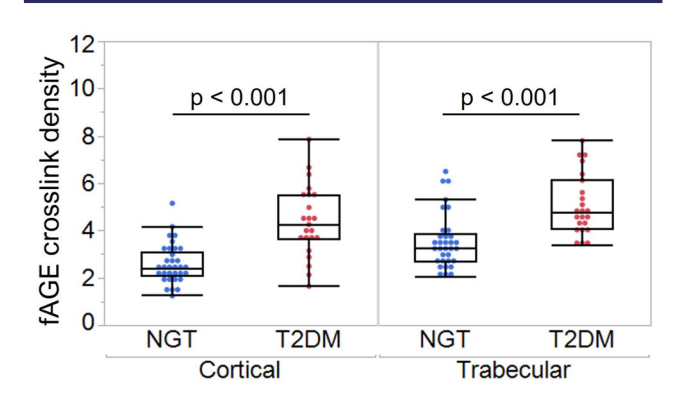


Fig. 4. Box plots of mean fAGE cross-link density in cortical and trabecular bone. fAGE cross-link density = mean two-photon fluorescence intensity normalized to the square root of mean SHG intensity. (67,74) Each overlaid jittered point represents the mean of the parameter from all three cortical or trabecular regions of interest per sample. The p values are obtained from linear mixed models adjusted by Tukey's HSD. fAGEs = fluorescent advanced glycation endproducts; NGT = normal glucose tolerance; T2DM = type 2 diabetes mellitus.

telopeptide of type 1 collagen (CTX), a marker of bone resorption, was 31% lower (p=0.043) compared with the NGT group. Additionally, P1NP was 24% lower (p=0.014) in the T2DM group compared with the IGT group. Undercarboxylated osteocalcin (ucOC) was 25% lower in the T2DM group compared with the NGT group (p=0.027). ucOC did not correlate with fasting plasma glucose levels or HbA1c. No differences were found among the groups in the serum levels of 25-hydroxyvitamin D, creatinine, calcium, phosphorous, sclerostin, or pentosidine.

High-performance liquid chromatography

Bone from the T2DM group had a higher concentration of the nonenzymatic cross-link pentosidine versus the NGT group in both cortical (+40%, p=0.003) and trabecular compartments (+35%, p=0.004). Further, trabecular bone of the T2DM group had a higher concentration of pentosidine versus the IGT group (+35%, p=0.007) and a similar trend existed in the cortical bone (+24%, p=0.087) (Fig. 2). The concentration of pentosidine was similar across the NGT and IGT groups in cortical and trabecular bone.

The concentrations of the enzymatic cross-links Pyd and Dpd did not differ across groups (Supplemental Table S2). The ratio of nonenzymatic cross-links to enzymatic cross-links (representing the ratio of harmful cross-links to advantageous cross-links), (73) measured as pentosidine/(Pyd + Dpd), was higher in T2DM specimens compared with NGT specimens in cortical bone (+33%, p=0.018) and trended toward being higher in T2DM specimens compared with IGT specimens (+27%, p=0.077). These differences did not persist in trabecular bone.

Multiphoton microscopy (MPM)

Bone from the T2DM group had a greater fAGE cross-link density compared with the NGT group (cortical +71%, p < 0.001; trabecular +44%, p < 0.001) (Figs. 3 and 4). Further, bone from the T2DM group had a greater mean normalized fluorescent AGE

Table 3. Comparisons of Nanoindentation Outcomes (Mean \pm Standard Deviation) in NGT and T2DM Groups in Cortical and Trabecular Bone Stratified by Tissue Region

Parameter	NGT	T2DM	% Difference versus NGT	<i>p</i> Value (NGT versus T2DM
Indentation Modulus (GPa)				
Cortical bone	15.4 \pm 3.18	16.8 ± 3.16	9	0.021
Osteonal bone	$\textbf{15.2} \pm \textbf{3.22}$	16.3 ± 3.15	7	0.252
Interstitial bone	15.5 ± 3.06	17.3 ± 3.10	12	0.035
Trabecular bone	14.3 ± 2.87	14.0 \pm 2.71	-2	0.482
Label	13.0 ± 2.96	12.7 ± 2.36	-2	0.992
Edge	14.5 ± 2.80	13.9 ± 2.70	-4	0.921
Center	15.5 ± 2.46	15.3 ± 2.42	-1	0.999
Hardness (GPa)				
Cortical bone	0.498 ± 0.0997	0.538 ± 0.107	8	0.039
Osteonal bone	0.497 ± 0.105	0.526 ± 0.107	6	0.434
Interstitial bone	0.498 ± 0.0815	0.551 ± 0.106	11	0.062
Trabecular bone	0.495 ± 0.0934	0.480 ± 0.0931	-3	0.473
Label	0.482 ± 0.108	0.471 ± 0.0916	-2	0.995
Edge	0.486 ± 0.0875	0.462 ± 0.0913	-5	0.862
Center	0.516 ± 0.0848	0.509 ± 0.0902	-1	0.999

NGT = normal glucose tolerance group; T2DM = type 2 diabetes mellitus group.

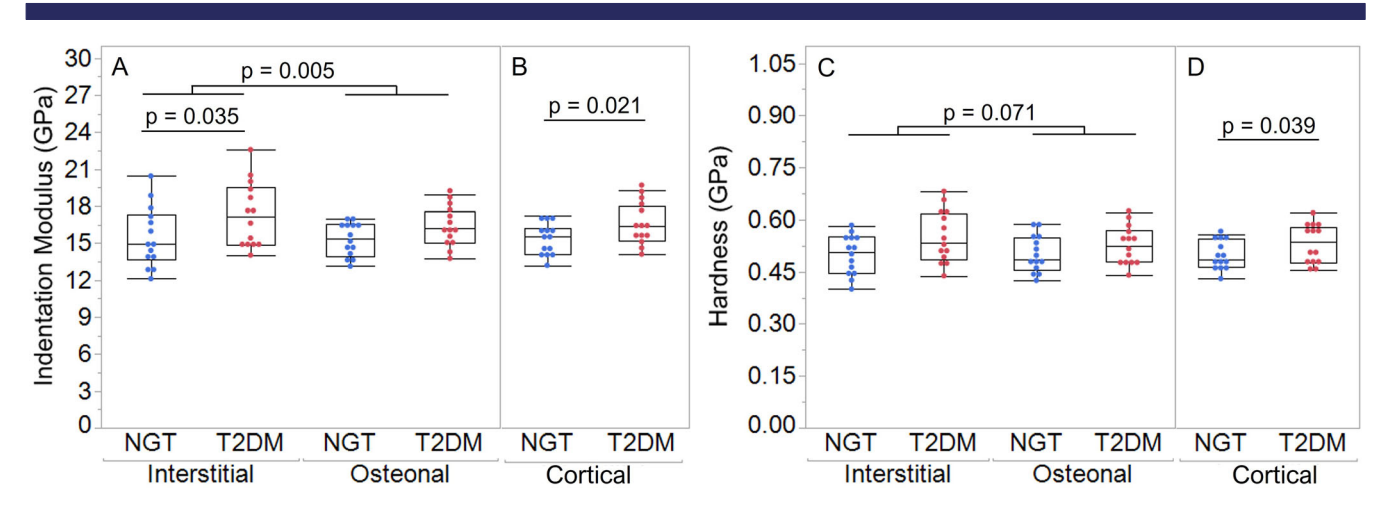


Fig. 5. Box plots of nanoindentation outcomes in cortical bone plotted by study group and tissue region: (*A*) indentation modulus and (*C*) hardness. Each overlaid jittered point represents the average value of 8 interstitial or 30 osteonal measurements per specimen. Specimen-average values (38 measurements per sample) of cortical (*B*) indentation modulus and (*D*) hardness by study group. The *p* values are obtained from linear mixed models adjusted by Tukey's HSD. NGT = normal glucose tolerance; T2DM = type 2 diabetes mellitus. All groupwise differences are indicated on the plots. A full list of region comparisons and *p* values are shown in Table 3 and Supplemental Table S3.

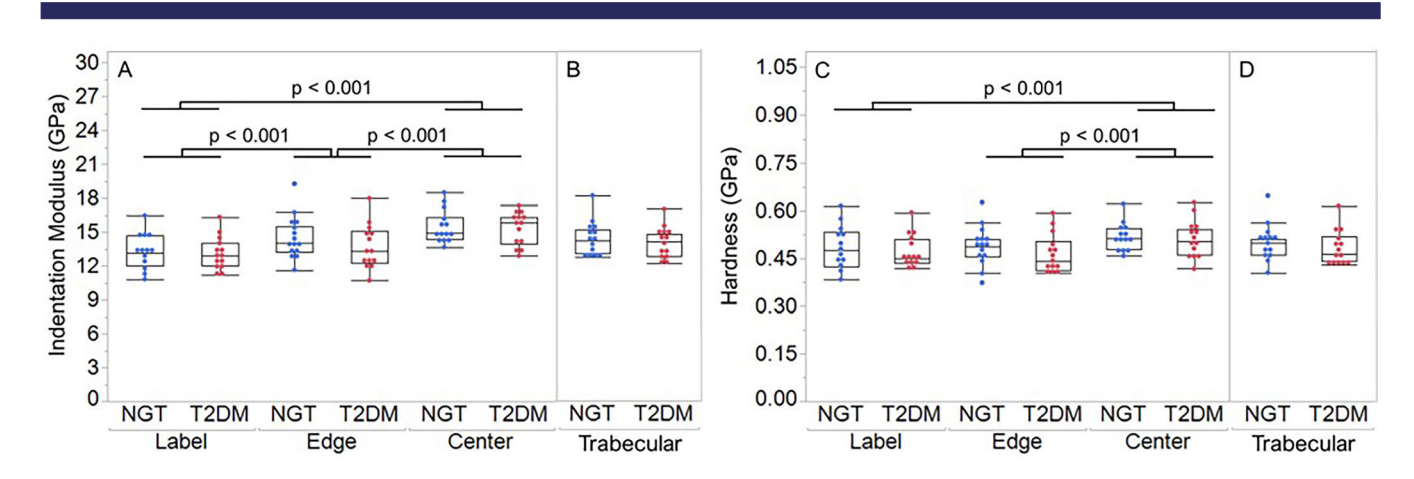


Fig. 6. Box plots of nanoindentation outcomes in trabecular bone plotted by study group and tissue region: (A) indentation modulus and (C) hardness. Each overlaid jittered point represents the average value of 10 measurements in either label or edge or center regions per specimen. Specimen-average values (30 measurements per sample) of trabecular (B) indentation modulus and (D) hardness by study group. The p values are obtained from linear mixed models adjusted by Tukey's HSD. NGT = normal glucose tolerance; T2DM = type 2 diabetes mellitus. All groupwise differences are indicated on the plots. A full list of region comparisons and p values are shown in Table 3 and Supplemental Table S3.

content compared with the NGT group (cortical +77%, p < 0.001; trabecular +57%, p < 0.001) (Supplemental Fig. S2A, C).

Qualitatively, the relatively older tissue (interstitial bone in the cortical compartment and the center of the trabeculae) had higher fAGE content compared with the younger tissue (Fig. 3).

Additionally, bone from the T2DM group had more variable fAGE content, as evidenced by the greater standard deviation of fluorescence intensity compared with that from the NGT group (cortical +54%, p < 0.001; trabecular +32%, p < 0.001) (Supplemental Fig. S2B, D).

First- and second-order statistical parameters of collagen organization in both cortical and trabecular bone were not different between T2DM and NGT groups (data not shown).

Nanoindentation

In cortical bone, the T2DM group had a higher indentation modulus (+9%, p=0.021) and hardness compared with the NGT group (+8%, p=0.039) (Table 3; Fig. 5B, D). Further, when material properties were analyzed within regions of the cortex, T2DM interstitial bone was stiffer (+4%, p=0.005) and trended toward being harder than osteonal bone (+2%, p=0.071) (Fig. 5A, C). This trend was observed only in the T2DM group but not in the NGT group. Additionally, the osteonal tissue had similar material properties between the groups.

In trabecular bone, indentation modulus and hardness did not differ with study group (Table 3; Fig. 6B, D). As expected, the

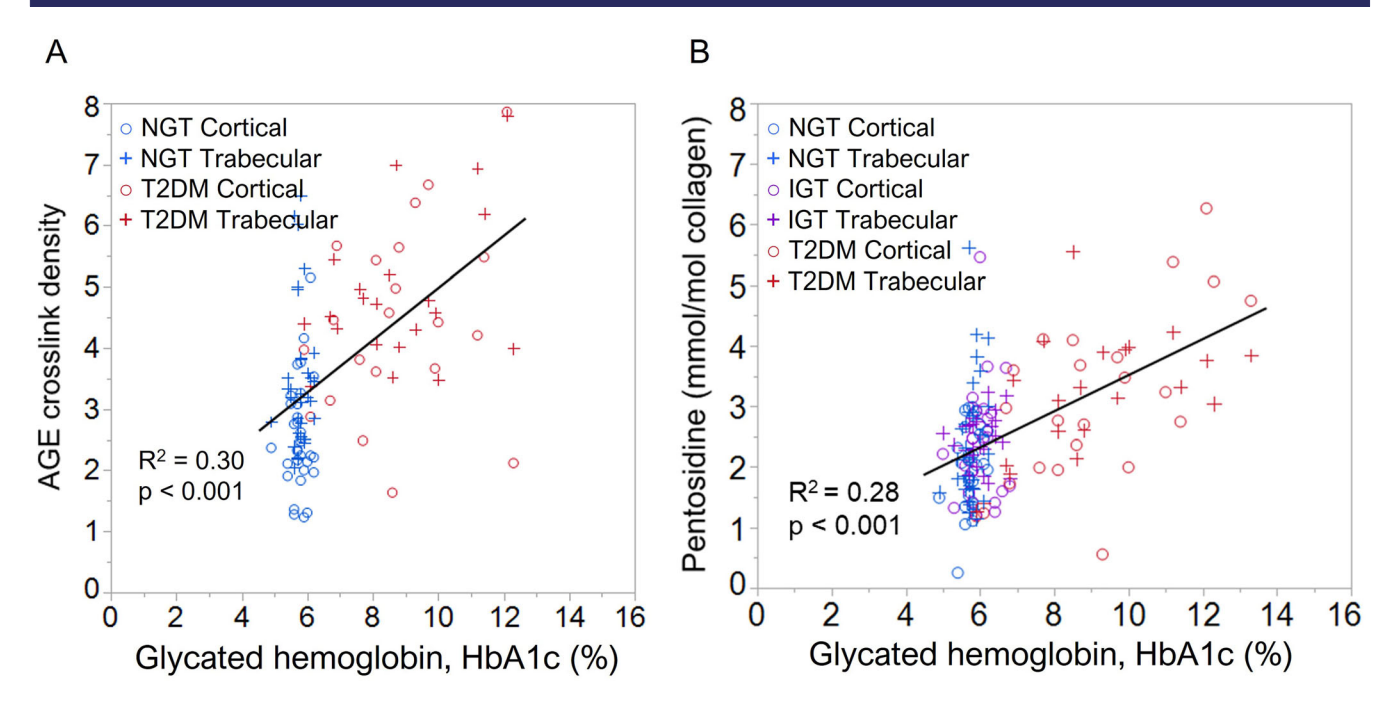


Fig. 7. (*A*) Relationship between fAGE cross-link density and HbA1c in cortical and trabecular bone. (*B*) Relationship between pentosidine content and HbA1c in cortical and trabecular bone. fAGE cross-link density = mean two-photon fluorescence intensity normalized to the square root of mean SHG intensity. Each open circle or plus symbol indicates the mean of fluorescent AGE content determined by averaging the fAGE content obtained from all the three MPM images taken per compartment per sample (*A*) or pentosidine content (*B*) per sample. NGT = normal glucose tolerance; T2DM = type 2 diabetes mellitus; AGE = advanced glycation endproducts.

Table 4. Final Regression Models of Sample Averaged Nanomechanical Organized by Patient Characteristics and Sample Averaged Compositional Properties

positionalitoperties					
	Cortic	al bone	Trabecu	Trabecular bone	
	Modulus (GPa)	Hardness (GPa)	Modulus (GPa)	Hardness (GPa)	
Race (black)	-	-0.03 (0.01)	-1 (0.2)	-0.03 (0.01)	
HbA1c (%)	0.26 (0.12)	0.016 (0.0049)	-	-	
P1NP (ng/mL)	-	-	0.03 (0.01)	-	
M:M (unitless)	-	-	5.7 (1.6)	0.14 (0.085)	
MMC (unitless)	1634 (536.2)	-	-	-	
C:P (unitless)	-	-	24 (3.9)	0.64 (0.21)	
Adjusted R ²	0.353	0.287	0.631	0.266	

Note: Values are shown as parameter coefficients with standard error in parentheses. Regression coefficients were determined from backward stepwise regressions using the minimum Akaike information criterion (AICc).

Abbreviations: P1NP = amino-terminal propeptide of type 1 collagen; M:M = mineral to matrix ratio; MMC = mineral maturity/crystallinity; C:P = carbonate to phosphate ratio.

center of the trabecula was stiffer and harder compared with tissue at the formation label and the edge (indentation modulus: +19% versus label, +8% versus edge; hardness: +8% versus label, +8% versus edge; all p < 0.001). Further, the edge of the trabecula was stiffer compared with tissue at the formation label (indentation modulus +10%, p < 0.001) (Fig. 6A). These trends in region material properties persisted in both NGT and T2DM groups (Supplemental Table S3).

Raman spectroscopy

In cortical bone, none of the Raman compositional parameters were different with study group. Across NGT and T2DM groups,

composition varied across osteonal and interstitial regions. Specifically, interstitial bone had higher mineral to matrix ratio and mineral maturity/crystallinity compared with osteonal bone (M:M +6%, p < 0.001; MMC +1%, p < 0.001) (Supplemental Fig. S3A, B). No differences were observed in carbonate to phosphate ratio with tissue region (Supplemental Fig. S3C). Additionally, in the T2DM group only, the interstitial bone had higher pyridinoline content (+6%, p < 0.001). Glycosaminoglycan content trended lower in interstitial bone compared with the osteonal bone (GAG -4%, p = 0.077) (Supplemental Figs. S3D and S5A).

In trabecular bone, none of the Raman compositional parameters were different with study group. Across NGT and T2DM groups, composition varied within trabecular regions.

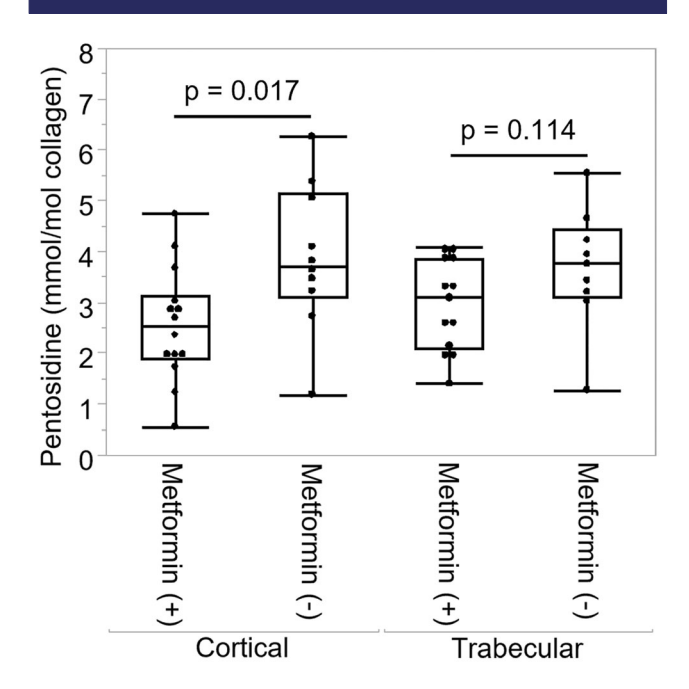


Fig. 8. Box plots of bone tissue pentosidine concentration in patients with T2DM who took metformin (metformin [+]) and who did not take metformin (metformin [-]). Each overlaid jittered point represents measured (raw data) pentosidine concentration in cortical or trabecular bone per specimen. The p values are obtained from standard least squares regression.

Specifically, the center of the trabecula had greater mineral to matrix ratio, mineral maturity/crystallinity, and carbonate to phosphate ratio compared with the edges (M:M +6%, p < 0.001; MMC +0.4%, p = 0.080; C:P +15%, p < 0.001) (Supplemental Fig. S4A-C). Further, tissue at the center and the edge of the trabecula had higher carbonate to phosphate ratio compared with that at the fluorochrome label (+21% versus center, p < 0.001; +5% versus edge, p = 0.064). The trends in mineral content were found only in the T2DM group but not in the NGT group. The trends in crystallinity persisted in both NGT and T2DM groups except the comparisons between edge and label regions, which were not significant. The center of the trabecula had higher pyridinoline content compared with the edge (+8%, p = 0.002) and label (+12%, p < 0.001) regions (Supplemental Fig. S4D). Additionally, the edge of the trabecula had lower GAG content compared with the label (-7%, p = 0.032) (Supplemental Fig. S5B). The GAG content was higher in the center of the trabecula compared with the edge (+10%, p = 0.015).

Relationships among glycemic control, medication use, compositional properties, and mechanical properties

When compositional properties were examined as a function of glycemic control, the AGE pentosidine assessed by HPLC and fAGE cross-link density assessed by multiphoton imaging increased with HbA1c (Pen: $R^2 = 0.28$, p < 0.001; fAGE cross-link density: $R^2 = 0.30$, p < 0.001) (Fig. 7). When these relationships were examined separately for cortical and trabecular bone, the slopes of the cortical and trabecular regression lines were not

different (p > 0.05). Pentosidine concentration weakly correlated with the average fAGE cross-link density ($R^2 = 0.20$, p < 0.001).

All the women with T2DM took insulin, but the individuals who also took metformin had lower pentosidine concentration in the cortical bone compared with individuals who did not take metformin (cortical -35%, p=0.017; trabecular -20%, p=0.114) (Fig. 8). However, metformin use did not affect fAGE cross-link density or other mechanical and compositional outcomes. P1NP was lower in individuals with T2DM taking metformin versus individuals with T2DM not taking metformin (-28%, p=0.007).

Relationships between specimen-averaged mechanical and compositional properties and patient characteristics (age, BMI, race, HbA1c, CTX, P1NP) were examined using backward stepwise regression models with minimum akaike information criterion (AICc) as stopping criterion. In cortical bone, indentation modulus and hardness increased with HbA1c. In trabecular bone, indentation modulus and hardness increased with mineral to matrix ratio and carbonate to phosphate ratio. Full list of parameters and their regression coefficients are listed in Table 4.

Relationships between spatially matched mechanical and compositional properties were examined using regression modeling adjusted for repeated measures (Supplemental Table S5). In both cortical and trabecular bone, indentation modulus and hardness increased with mineral maturity/crystallinity and/or carbonate to phosphate ratio. Finally, no relationships were observed between mechanical properties assessed by nanoindentation and fAGE cross-link density or pentosidine.

Discussion

In this study, we measured compositional and nanomechanical properties of iliac cortical and trabecular bone from postmeno-pausal women with NGT, IGT, and T2DM. As hypothesized, women with overt T2DM had higher cortical and trabecular AGE content compared with women with NGT, and the AGE content increased with HbA1c. Further, the cortical tissue from women with T2DM was stiffer and harder compared with that in women with NGT. Overall, compositional and mechanical properties of bone were altered in women with T2DM compared with those with NGT or IGT.

The T2DM group had reduced bone remodeling compared with the NGT group, as indicated by the serum markers of bone turnover. Specifically, the serum P1NP content, a marker of bone formation, and CTX content, a marker of bone resorption, were lower in the T2DM group compared with the NGT group; P1NP was also lower in the T2DM group compared with the IGT group but did not differ between NGT and IGT groups. These results suggest that bone formation is reduced during the transition from prediabetes to T2DM but remains unaltered as normal glycemic control progresses to prediabetes. At the same time, bone resorption declines during the transition from NGT through T2DM. This loss in resorption before reduction in formation may explain the preserved or increased BMD in individuals with T2DM. Additionally, higher BMI observed in the T2DM group may contribute to the preserved to higher BMD in these individuals. Overall, these results are in accordance with prior histomorphometric and serum studies showing that individuals with T2DM have reduced bone remodeling compared with nondiabetic individuals. (20,21,23,75)

Serum and urinary biomarkers indicated as potential tools for diagnosis of T2DM showed variable trends with T2DM status.

ucOC was lower in the T2DM group compared with the NGT group, consistent with previous studies. (76-78) Further, ucOC did not correlate with fasting plasma glucose levels, consistent with a previous study in postmenopausal women. (78) However, some studies that enrolled both men and women showed negative and weak $(R^2 < 0.2)$ correlations between ucOC and fasting plasma glucose levels and predicted cardiovascular and T2DM risk in individuals with metabolic syndrome. (76-82) In the current study, serum levels of ucOC were highly variable among groups (coefficient of variation: 0.6-0.9, Table 2). Because our study was not powered to identify relationships among these highly variable serum metrics, we did not detect the weak correlations between ucOC and fasting plasma glucose levels observed in some prior work. Serum pentosidine content was not different among the groups potentially because of weak correlations between bone pentosidine and serum pentosidine. (26,83) A previous study on individuals with T2DM also reported no differences in serum pentosidine content, (26) and another study showed weak or nonsignificant correlations between serum and bone pentosidine. (83) This discrepancy may be attributed to the fact that bone turnover takes much longer than other collagenous tissues, which may result in lower contribution to the serum pentosidine from bone.

As hypothesized, both cortical and trabecular bone from the T2DM group had higher concentrations of the AGE pentosidine and total fluorescent AGEs compared with the NGT group. Pentosidine content in the IGT group was lower than that in the T2DM group but was not different from that in the NGT group, indicating that the greater AGE content observed in T2DM bone occurs as IGT progresses to T2DM. Enzymatic cross-link content was similar across the groups, indicating that AGEs may not interfere with the formation of enzymatic cross-links. Previous studies showed higher AGE content in cortical and trabecular bone in individuals with T2DM compared with non-DM individuals; (25-27,34,35,37) however, a few studies reported similar total fluorescent AGE content in T2DM trabecular bone. (25,26) Although previous studies have reported higher AGEs in individuals with T2DM, only one study found a correlation between HbA1c and trabecular bone AGEs, (34) whereas other studies did not observe any association between HbA1c and bone AGEs. (25,26)

To our knowledge, this is the first study to utilize semiquantitative multiphoton images of AGE concentration to provide spatially resolved maps of AGE accumulation in a T2DM population. This analysis showed that the relatively older tissue (interstitial bone in the cortical region and the center of the trabecula) had higher fAGE content compared with the younger tissue in both NGT and T2DM groups. Specifically, AGEs appear to accumulate in the less remodeled regions of bone, as evidenced by the large difference in AGE content in the relatively older regions versus younger regions in the T2DM group compared with the NGT group (Fig. 3). This variation in AGE concentration within images was reflected in the greater standard deviation of fluorescence intensity in the T2DM compared with the NGT group (Supplemental Fig. S2).

AGE accumulation is a time-dependent process as evidenced by increased AGE content with longer duration of glucose incubation in in vitro studies. (47) The longer the tissue is present in the body, the higher the AGE concentration, which along with lower turnover in individuals with T2DM, contributes to the preferential accumulation of AGEs in the interstitial bone and the center of trabeculae observed in the current study. Bone turnover rate further decreases with increasing age, diabetes duration, and other comorbidities, which may result in an increase

in the percentage of older tissue with high AGE content and consequently increase overall brittleness of the bone tissue. (29,84) Although a previous study showed that AGEs accumulate in the center of trabeculae, (85) to our knowledge, the current study is the first dedicated study to visualize spatial accumulation of AGEs in a clinical population of individuals with T2DM.

In this study, we measured total fAGEs and pentosidine, a fluorescent cross-link, which was selected for analysis because a serum assay for pentosidine is widely clinically available. Many other AGEs, such as carboxymethyl-lysine (CML), a nonfluorescent AGE, have been identified in bone and other tissues and may reflect or contribute to bone fragility. (86-88) In particular, greater CML concentration in bone is associated with decreased fracture toughness, although the mechanism through which a non-cross-linking AGE affects bone material properties remains unknown. (89) Nevertheless, pentosidine concentration strongly correlates with several quantifiable AGEs, including CML. (88) Therefore, fAGE content and pentosidine together are a practical surrogate for overall tissue AGE content.

Second harmonic generation images of collagen were obtained to study the effects of the altered cross-linking profile on the microscale structure of collagen. No differences were observed in the collagen content and organization in cortical or trabecular bone in the NGT or T2DM samples. Our results suggest that in adults with T2DM, changes in nonenzymatic cross-linking at molecular level do not alter microscale organization of collagen, which is controlled by osteoblastic cellular function, enzymatic actions, and gene expression. (90-93)

The nanomechanical properties were altered in cortical bone but preserved in trabecular bone in the T2DM group compared with the NGT group. The T2DM group had stiffer and harder cortices compared with the NGT group. In cortical bone, only the interstitial tissue was stiffer and trended toward higher hardness in the T2DM group compared with that in the NGT group. Osteonal tissue, or relatively newer tissue, had similar material properties between the groups. This result may explain why a previous study that characterized only osteonal bone did not observe any differences in nanomechanical properties of T2DM bone versus non-DM bone. (37) Additionally, when the NGT and T2DM group data was pooled, the interstitial region was stiffer and harder compared with the osteonal regions, consistent with previous studies. (54,94,95)

Conversely, the trabecular bone mechanical properties were not different among the groups but showed consistent trends by region, consistent with previous studies⁽⁹⁶⁾: the central region was hardest and stiffest; the edge had intermediate values; and the label region was softest and most compliant. A previous study on trabecular bone reported lower indentation modulus and hardness in individuals with T2DM compared with non-DM individuals. (34) Although the trend is similar in the current study, the differences between groups are not statistically significant. Unfortunately, the current study was not designed to address the underlying causes for the compartment-specific effects of T2DM on nanomechanical properties. Factors that may contribute to preserved nanomechanical properties in trabecular bone versus altered properties in cortical bone in individuals with T2DM include higher turnover, which replaces bone tissue faster in trabecular bone versus cortical bone, (97) and higher surface area, which allows greater osteoclastic activity. (98,99) Therefore, trabecular bone may be less susceptible to deleterious changes because of T2DM as evidenced by preserved mechanical properties and a smaller increase in AGEs compared with cortical bone observed in this study. Overall, these results indicate that the

cortex had more profound changes in material properties than cancellous tissue.

In both cortical and trabecular bone, Raman compositional outcomes did not differ with the study group but were consistent with relative tissue age. GAG content was similar between the T2DM and the NGT groups. GAG content was higher at the center compared with the edge of the trabecula, consistent with prior studies. (100,101) DM was associated with deleterious changes in GAG structure and function in kidney, liver, blood vessels, and other tissues. (102,103) The Raman GAG peak has a low signal to noise ratio, and this outcome is not as extensively validated in bone as other parameters in Table 1. (104) Therefore, dedicated studies using gold standard techniques are required to confirm the effects of T2DM on bone GAG structure and function. Although higher mineralization in individuals with T2DM versus non-DM individuals was reported previously in FTIR analyses in trabecular bone (25,36) and in cortical bone in the full cohort from this study, (38) no differences in bone composition with T2DM were found in the current study. The smaller sample size and characterization area (18 point spectra in cortical bone, 27 spectra in trabecular bone per sample) selected to aid correlation of mechanical and compositional properties in the current study, as well as the differences in Raman and FTIR vibrational techniques, (104) may be responsible for the lack of differences observed. The trends in the compositional outcomes with region are generally consistent with the expected properties of recently formed versus older tissue and agree well with previous studies. (100,101,105)

When relationships among glycemic control and bone tissue composition were examined, regression analysis revealed that poor glycemic control is associated with accumulation of bone tissue AGEs. In this study, AGE content was not a significant explanatory variable for the material properties of the bone, suggesting that AGEs do not directly affect the microscale indentation modulus or hardness of the bone. This result is expected as the mineral component predominantly dictates elastic properties, and the collagen cross-linking dictates postvield properties. (106,107) Surprisingly, mineral content was not associated with indentation modulus or hardness, but mineral maturity/crystallinity positively correlated with indentation modulus in cortical bone and carbonate to phosphate ratio positively correlated with indentation modulus in trabecular bone. These results indicate that larger and/or more imperfect crystals increase tissue stiffness. Previous studies reported a similar relationship between mineral crystallinity and indentation modulus, (104,108) but the mechanism through which large and/or imperfect crystals increase stiffness is unknown. (109)

In addition to the deleterious effects of glycemic derangement on bone, diabetic medications such as insulin and metformin can also independently affect bone properties. (110,111) Insulin is generally considered to have anabolic effects on bone, supporting the hypothesis that hyperinsulinemia in T2DM contributes to preserved or increased BMD in these individuals. (112,113) However, the persistent higher fracture risk in T2DM individuals on insulin therapy indicates that the positive effects of insulin on BMD do not fully compensate for the deleterious effects of T2DM on bone material properties. (4,9,17)

Individuals with T2DM taking metformin and insulin had lower bone pentosidine concentration compared with individuals taking only insulin. Metformin is thought to decrease AGEs by reducing AGE receptors (RAGEs) and by stimulation of catabolic pathways produced through metformin mechanism of action.⁽¹⁸⁾ Previous in vitro studies on rat osteoblasts showed metformin treatment can reverse the deleterious effects of AGEs

on these cells. (114,115) Further, P1NP was reduced in individuals with T2DM taking metformin compared with individuals with T2DM not on metformin similar to the results from a previous study. (116) Further dedicated studies are required to understand the effects of metformin on bone tissue properties and its mechanism of action. To our knowledge, this is the first study to report the effects of metformin on bone AGE content in a clinical population.

Although the precise mechanism underlying diabetic bone fragility is unknown, emerging evidence suggests that reduction in post-yield strain because of accumulation of AGEs may contribute to brittle bones in individuals with T2DM. Previous in vitro glycation studies showed that AGE accumulation degrades post-yield properties and increases residual stress in the bone matrix. (84,117-119) These in vitro data are reinforced by the recent evidence from studies of (i) T2DM rat model showing reduced collagen fibrillar sliding, which is an intrinsic toughening mechanism, (120) and (ii) clinical specimens of cancellous bone from individuals with T2DM showing reduced post-yield strain with AGE accumulation. (25,34) In this study, we showed that individuals with T2DM on insulin have higher pentosidine compared with individuals with NGT and IGT and higher fAGE density compared with individuals with NGT in both cortical and trabecular bone. Although previous studies have reported higher bone AGE content in individuals with T2DM, the results were limited to a single compartment (either cortical or trabecular bone).

Additionally, our results refine our understanding of the timing of these changes in bone quality by showing that AGEs increase in transition from IGT to overt T2DM. Our study is the first to consider accumulation of AGEs with progression of glycemic derangement as a potential mechanism for increased fracture risk in individuals with T2DM but not in individuals with IGT. In characterizing different stages of diabetes and quantifying AGE content through each skeletal stage, we were able to ground clinical observation in a potential pathophysiologic mechanism for bone fragility in overt T2DM.

This study has several key strengths and limitations. The strengths of this study include recruitment of individuals with NGT, IGT, and overt T2DM to study the effects of increasing disease severity on bone quality. Our criterion to include women with T2DM on insulin (i) ensured that participants who are indicated for insulin treatment received it, thereby excluding effects of untreated disease/unmitigated hyperglycemia and (ii) addressed limitations of prior studies. Specifically, previous studies characterizing bone material properties in clinical specimens from individuals with T2DM did not take into account or control for the disease severity or duration. (25,26,34,35,37) We provided the first spatially resolved quantification of AGEs, mechanical, and compositional properties of bone from individuals with T2DM. To our knowledge, this is the first study to report nanomechanical properties at fluorochrome label region in human biopsies. The limitations of this study are that the iliac crest is not a clinically relevant fracture site, and it is unknown if the changes in bone quality with T2DM are systemic. The cross-sectional study design precluded longitudinal monitoring of the subjects, which may have provided more precise information on the timing of the changes observed in this study. The IGT group was not characterized with nanoindentation and Raman spectroscopy because no differences in BMD and bone turnover markers in NGT versus IGT groups were observed, which is expected to reflect similar extent of secondary mineralization, and comparable stiffness. Double fluorochrome labels could not be resolved in the thick, embedded bone, which otherwise could have provided more tightly controlled regions of

known tissue age. Nevertheless, this study is the first to provide information on nanoscale bone material properties in both cortical and trabecular bone from the same cohort and the effect of relative tissue age on spatial distribution of AGEs in individuals with T2DM.

The discordance between bone density and fracture risk in T2DM remains incompletely understood. In this study, we have uniquely shown that there are differences in AGE content as well as nanomechanical properties in bone from postmenopausal women with NGT, IGT, and T2DM. Bone tissue AGEs, which have previously been shown to embrittle bone, (25,34,84,117-119) increased with worsening glycemic control. This relationship suggests a potential mechanism by which bone fragility may increase despite greater tissue stiffness and hardness in individuals with T2DM; our results suggest that it occurs in the transition from IGT to overt T2DM.

Conflicts of Interest

The authors declare no conflicts of interest.

Acknowledgments

We thank Dr Shefford Baker, Zach Rouse, and Ziyue Yao for assistance with nanoindentation and Johanna M Dela Cruz for assistance with multiphoton imaging.

Imaging data were acquired through the Cornell University Biotechnology Resource Center, with NIH S100D018516 funding for the shared Zeiss LSM880 confocal/multiphoton microscope.

This work made use of the Cornell Center for Materials Research Shared Facilities, which are supported through the NSF MRSEC program (DMR-1719875).

Author Contributions

Sashank Lekkala: Data curation; formal analysis; investigation; methodology; validation; visualization; writing – original draft; writing – review and editing. Sara E. Sacher: Data curation; formal analysis; methodology; validation; writing – original draft; writing – review and editing. Erik Arthur Taylor: Methodology; validation; writing – review and editing. Rebecca M. Williams: Data curation; methodology; writing – review and editing. Kendall F Moseley: Conceptualization; data curation; formal analysis; funding acquisition; investigation; writing – review and editing. Eve Donnelly: Conceptualization; writing – review and editing. Eve Donnelly: Conceptualization; methodology; project administration; resources; supervision; validation; visualization; writing – review and editing.

Peer Review

The peer review history for this article is available at https://publons.com/publon/10.1002/jbmr.4757.

Data Availability Statement

The data that support the findings of this study are available in the supplementary material of this article and are available from the corresponding author upon reasonable request.

References

- Vestergaard P. Discrepancies in bone mineral density and fracture risk in patients with type 1 and type 2 diabetes - a meta-analysis. Osteoporos Int. 2007;18(4):427-444.
- Janghorbani M, Van Dam RM, Willett WC, Hu FB. Systematic review of type 1 and type 2 diabetes mellitus and risk of fracture. Am J Epidemiol. 2007;166(5):495-505.
- 3. Schwartz AV. Epidemiology of fractures in type 2 diabetes. Bone. 2016:82:2-8.
- 4. Schwartz AV, Vittinghoff E, Bauer DC, et al. Association of BMD and FRAX score with risk of fracture in older adults with type 2 diabetes. JAMA. 2011;305(21):2184-2192.
- Bonds DE, Larson JC, Schwartz AV, et al. Risk of fracture in women with type 2 diabetes: the Women's Health Initiative Observational Study. J Clin Endocrinol Metabol. 2006;91(9):3404-3410.
- Starup-Linde J, Frost M, Vestergaard P, Abrahamsen B. Epidemiology of fractures in diabetes. Calcif Tissue Int. 2017;100(2):109-121.
- 7. Nathan DM, Davidson MB, DeFronzo RA, et al. Impaired fasting glucose and impaired glucose tolerance: implications for care. Diabetes Care. 2007;30:753-759.
- 8. De Liefde II, Van Der Klift M, De Laet CEDH, Van Daele PLA, Hofman A, Pols HAP. Bone mineral density and fracture risk in type-2 diabetes mellitus: the Rotterdam study. Osteoporos Int. 2005;16(12):1713-1720.
- 9. Napoli N, Strotmeyer ES, Ensrud KE, et al. Fracture risk in diabetic elderly men: the MrOS study. Diabetologia. 2014;57(10):2057-2065.
- Strotmeyer ES, Cauley JA, Schwartz AV, et al. Nontraumatic fracture risk with diabetes mellitus and impaired fasting glucose in older white and black adults: the Health, Aging, and Body Composition Study. Arch Intern Med. 2005;165(14):1612-1617.
- Napoli N, Chandran M, Pierroz DD, Abrahamsen B, Schwartz AV, Ferrari SL. Mechanisms of diabetes mellitus-induced bone fragility. Nat Rev Endocrinol. 2017;13(4):208-219.
- Hamann C, Kirschner S, Günther KP, Hofbauer LC. Bone, sweet bone

 osteoporotic fractures in diabetes mellitus. Nat Rev Endocrinol. 2012;8(5):297-305.
- Shanbhogue VV, Mitchell DM, Rosen CJ, Bouxsein ML. Type 2 diabetes and the skeleton: new insights into sweet bones. Lancet Diabetes Endocrinol. 2016;4(2):159-173.
- Turner R, Cull C, Holman R. United Kingdom prospective diabetes study 17: a 9-year update of a randomized, controlled trial on the effect of improved metabolic control on complications in non-insulin-dependent diabetes mellitus. Ann Intern Med. 1996;124(1 Pt 2): 136-145.
- Franch-Nadal J, Roura-Olmeda P, Benito-Badorrey B, Rodriguez-Poncelas A, Coll-de-Tuero G, Mata-Cases M. Metabolic control and cardiovascular risk factors in type 2 diabetes mellitus patients according to diabetes duration. Fam Pract. 2015;32(1):27-34.
- Hayashino Y, Izumi K, Okamura S, Nishimura R, Origasa H, Tajima N. Duration of diabetes and types of diabetes therapy in Japanese patients with type 2 diabetes: the Japan Diabetes Complication and Its Prevention Prospective Study 3 (JDCP study 3). J Diabetes Investig. 2017;8(2):243.
- 17. Losada-Grande E, Hawley S, Soldevila B, et al. Insulin use and excess fracture risk in patients with type 2 diabetes: a propensity-matched cohort analysis. Sci Rep. 2017;7(1):1-9.
- Bahrambeigi S, Yousefi B, Rahimi M, Shafiei-Irannejad V. Metformin; an old antidiabetic drug with new potentials in bone disorders. Biomed Pharmacother. 2019;109:1593-1601.
- Wang LX, Wang GY, Su N, Ma J, Li YK. Effects of different doses of metformin on bone mineral density and bone metabolism in elderly male patients with type 2 diabetes mellitus. World J Clin Cases. 2020;8(18):4010.
- Manavalan JS, Cremers S, Dempster DW, et al. Circulating osteogenic precursor cells in type 2 diabetes mellitus. J Clin Endocrinol Metab. 2012;97(9):3240-3250.

15234681, 2023. 2, Downloaded from https://asbmr.onlinelibrary.wiley.com/doi/10.1002/jbmr.4757 by Comell University, Wiley Online Library on [08/02/2023]. See the Terms and Conditions (https://onlinelibrary.wiley.com/ onditions) on Wiley Online Library for rules of use; OA articles are governed by the applicable Creative Commons License

- 21. Krakauer JC, McKenna MJ, Buderer NF, Rao DS, Whitehouse FW, Parfitt AM. Bone loss and bone turnover in diabetes. Diabetes. 1995:44(7):775-782.
- 22. Starup-Linde J, Vestergaard P. Biochemical bone turnover markers in diabetes mellitus - a systematic review. Bone. 2016;82:69-78.
- 23. Hygum K, Starup-Linde J, Harsløf T, Vestergaard P, Langdahl BL. Diabetes mellitus, a state of low bone turnover-a systematic review and meta-analysis. Eur J Endocrinol. 2017;176(3):R137-R157.
- 24. Costantini S, Conte C. Bone health in diabetes and prediabetes. World J Diabetes. 2019;10(8):421-445.
- 25. Hunt HB, Torres AM, Palomino PM, et al. Altered tissue composition, microarchitecture, and mechanical performance in cancellous bone from men with type 2 diabetes mellitus. J Bone Miner Res. 2019; 34(7):1191-1206.
- 26. Karim L, Moulton J, Van Vliet M, et al. Bone microarchitecture, biomechanical properties, and advanced glycation end-products in the proximal femur of adults with type 2 diabetes. Bone. 2018; 114(May):32-39.
- 27. Bucknell A, King KB, Oren TW, Botolin S, Williams A. Arthroplasty in veterans: analysis of cartilage, bone, serum, and synovial fluid reveals differences and similarities in osteoarthritis with and without comorbid diabetes, J Rehabil Res Dev. 2012;48(10):1195.
- 28. Kida Y, Saito M, Shinohara A, Soshi S, Marumo K. Non-invasive skin autofluorescence, blood and urine assays of the advanced glycation end product (AGE) pentosidine as an indirect indicator of AGE content in human bone. BMC Musculoskelet Disord. 2019;20(1):1-8.
- 29. Karim L, Tang SY, Sroga GE, Vashishth D. Differences in nonenzymatic glycation and collagen cross-links between human cortical and cancellous bone. Osteoporos Int. 2013;24(9):2441-2447.
- 30. Saito M, Fujii K, Mori Y, Marumo K. Role of collagen enzymatic and glycation induced cross-links as a determinant of bone quality in spontaneously diabetic WBN/Kob rats. Osteoporos Int. 2006; 17(10):1514-1523.
- 31. Saito M, Marumo K. Collagen cross-links as a determinant of bone quality: a possible explanation for bone fragility in aging, osteoporosis, and diabetes mellitus. Osteoporos Int. 2010;21:195-214.
- 32. Sassi F, Buondonno I, Luppi C, et al. Type 2 diabetes affects bone cells precursors and bone turnover. BMC Endocr Disord. 2018; 18(1):55.
- 33. Hunt HB. Characterization of material properties, microarchitecture, and mechanics of bone from subjects with type 2 diabetes mellitus (Order No. 13419141). Available from ProQuest Dissertations & Theses Global. (2169371366). 2018.
- 34. Sihota P, Yadav RN, Dhaliwal R, et al. Investigation of mechanical, material and compositional determinants of human trabecular bone quality in type 2 diabetes. J Clin Endocrinol Metab. 2021; 106(5):e2271-e2289.
- 35. Piccoli A, Cannata F, Strollo R, et al. Sclerostin regulation, microarchitecture, and advanced glycation end-products in the bone of elderly women with type 2 diabetes. J Bone Mineral Res. 2020; 35(12):2415-2422.
- 36. Pritchard JM, Papaioannou A, Tomowich C, et al. Bone mineralization is elevated and less heterogeneous in adults with type 2 diabetes and osteoarthritis compared to controls with osteoarthritis alone. Bone. 2013;54(1):76-82.
- 37. Wölfel EM, Jähn-Rickert K, Schmidt FN, et al. Individuals with type 2 diabetes mellitus show dimorphic and heterogeneous patterns of loss in femoral bone quality. Bone. 2020;140:115556.
- 38. Hunt HB, Miller NA, Hemmerling KJ, et al. Bone tissue composition in postmenopausal women varies with glycemic control from normal glucose tolerance to type 2 diabetes mellitus. J Bone Mineral Res. 2021;36(2):334-346.
- 39. Pritchard JM, Papaioannou A, Schwarcz HP, et al. A comparison of collagen crosslink content in bone specimens from elective total hip arthroplasty patients with and without type 2 diabetes. J Bone Res Rep. 2016;2(3):3.
- 40. Ionova-Martin SS, Wade JM, Tang S, et al. Changes in cortical bone response to high-fat diet from adolescence to adulthood in mice. Osteoporos Int. 2011;22(8):2283-2293.

- 41. Farr JN, Drake MT, Amin S, Melton LJ, McCready LK, Khosla S, In vivo assessment of bone quality in postmenopausal women with type 2 diabetes. J Bone Miner Res. 2014:29(4):787-795.
- 42. Nilsson AG, Sundh D, Johansson L, et al. Type 2 diabetes mellitus is associated with better bone microarchitecture but lower bone material strength and poorer physical function in elderly women: a population-based study. J Bone Miner Res. 2017;32(5):1062-1071.
- 43. Furst JR, Bandeira LC, Fan WW, et al. Advanced glycation endproducts and bone material strength in type 2 diabetes. J Clin Endocrinol Metabol. 2016;101(6):2502-2510.
- 44. Parle E, Tio S, Behre A, et al. Bone mineral is more heterogeneously distributed in the femoral heads of osteoporotic and diabetic patients: a pilot study. JBMR Plus. 2020;4(2):e10253.
- 45. Cohen A. Dempster DW. Müller R. et al. Assessment of trabecular and cortical architecture and mechanical competence of bone by high-resolution peripheral computed tomography: comparison with transiliac bone biopsy. Osteoporos Int. 2010;21(2):263-273.
- 46. Boskey AL, Coleman R. Aging and bone. J Dent Res. 2010;89(12):
- 47. Vashishth D, Gibson GJ, Khoury JI, Schaffler MB, Kimura J, Fyhrie DP. Influence of nonenzymatic glycation on biomechanical properties of cortical bone. Bone. 2001;28(2):195-201.
- 48. Lloyd AA, Gludovatz B, Riedel C, et al. Atypical fracture with longterm bisphosphonate therapy is associated with altered cortical composition and reduced fracture resistance. Proc Natl Acad Sci U S A. 2017;114:8722-8727.
- 49. Donnelly E, Williams RM, Downs SA, Dickinson ME, Baker SP, van der Meulen MCH. Quasistatic and dynamic nanomechanical properties of cancellous bone tissue relate to collagen content and organization. J Mater Res. 2006;21(8):2106-2117.
- 50. Weber M, Roschger P, Fratzl-Zelman N, et al. Pamidronate does not adversely affect bone intrinsic material properties in children with osteogenesis imperfecta. Bone. 2006;39(3):616-622.
- 51. Kim G, Cole JH, Boskey AL, Baker SP, Van Der Meulen MCH. Reduced tissue-level stiffness and mineralization in osteoporotic cancellous bone. Calcif Tissue Int. 2014;95(2):125-131.
- 52. Donnelly E, Boskey AL, Baker SP, Van Der Meulen MCH. Effects of tissue age on bone tissue material composition and nanomechanical properties in the rat cortex. J Biomed Mater Res A. 2010;92(3):1048.
- 53. Boivin G, Farlay D, Bala Y, Doublier A, Meunier PJ, Delmas PD. Influence of remodeling on the mineralization of bone tissue. Osteoporos Int. 2009;20(6):1023-1026.
- 54. Lefèvre E, Farlay D, Bala Y, et al. Compositional and mechanical properties of growing cortical bone tissue: a study of the human fibula. Sci Rep. 2019;9(1):1-16.
- 55. Donnelly E, Baker SP, Boskey AL, Van Der Meulen MCH. Effects of surface roughness and maximum load on the mechanical properties of cancellous bone measured by nanoindentation. J Biomed Mater Res A. 2006;77(2):426-435.
- 56. Pharr GM. An improved technique for determining hardness and elastic modulus using load and displacement sensing indentation experiments. J Mater Res. 1992;7(6):1564-1583.
- 57. Polly BJ, Yuya PA, Akhter MP, Recker RR, Turner JA. Intrinsic material properties of trabecular bone by nanoindentation testing of biopsies taken from healthy women before and after menopause. Calcif Tissue Int. 2012;90(4):286-293.
- 58. Farlay D, Armas LAG, Gineyts E, Akhter MP, Recker RR, Boivin G. Nonenzymatic glycation and degree of mineralization are higher in bone from fractured patients with type 1 diabetes mellitus. J Bone Miner Res. 2016;31(1):190-195.
- 59. Ellis R, Green E, Winlove CP. Structural analysis of glycosaminoglycans and proteoglycans by means of Raman microspectrometry. Connect Tissue Res. 2009;50(1):29-36.
- 60. Gamsjaeger S, Klaushofer K, Paschalis EP. Raman analysis of proteoglycans simultaneously in bone and cartilage. J Raman Spectrosc. 2014;45(9):794-800.
- 61. Unal M, Uppuganti S, Leverant CJ, et al. Assessing glycationmediated changes in human cortical bone with Raman spectroscopy. J Biophotonics. 2018;11(8):e201700352.

ENDPRODUCTS 275 Journal of Bone and Mineral Research



- 62. Gamsjaeger S, Masic A, Roschger P, et al. Cortical bone composition and orientation as a function of animal and tissue age in mice by Raman spectroscopy. Bone. 2010;47(2):392-399.
- Kazanci M, Fratzl P, Klaushofer K, Paschalis EP. Complementary information on in vitro conversion of amorphous (precursor) calcium phosphate to hydroxyapatite from Raman microspectroscopy and wide-angle X-ray scattering. Calcif Tissue Int. 2006;79(5): 354-359.
- 64. Awonusi A, Morris MD, Tecklenburg MMJ. Carbonate assignment and calibration in the Raman spectrum of apatite. Calcif Tissue Int. 2007;81(1):46-52.
- 65. Gamsjaeger S, Robins SP, Tatakis DN, Klaushofer K, Paschalis EP. Identification of pyridinoline trivalent collagen cross-links by Raman microspectroscopy. Calcif Tissue Int. 2017;100(6):565-574.
- 66. Boyd RW. Nonlinear optics. San Diego: Academic Press; 2003 p 578.
- Marturano JE, Xylas JF, Sridharan GV, Georgakoudi I, Kuo CK. Lysyl oxidase-mediated collagen crosslinks may be assessed as markers of functional properties of tendon tissue formation. Acta Biomater. 2014;10(3):1370-1379.
- Monnier VM, Kohn RR, Cerami A. Accelerated age-related browning of human collagen in diabetes mellitus. Proc Natl Acad Sci U S A. 1984;81(2 I):583-587.
- Whitaker JE, Haugland RP, Moore PL, Hewitt PC, Reese M, Haugland RP. Cascade blue derivatives: water soluble, reactive, blue emission dyes evaluated as fluorescent labels and tracers. Anal Biochem. 1991:198(1):119-130.
- Dudenkova VV, Shirmanova MV, Lukina MM, Feldshtein FI, Virkin A, Zagainova EV. Examination of collagen structure and state by the second harmonic generation microscopy. Biochemistry. 2019;84-(Suppl 1):S89-S107.
- Bank RA, Beekman B, Verzijl N, De Roos JADM, Nico Sakkee A, Tekoppele JM. Sensitive fluorimetric quantitation of pyridinium and pentosidine crosslinks in biological samples in a single highperformance liquid chromatographic run. J Chromatogr B Biomed Appl. 1997;703(1–2):37-44.
- Bank RA, Jansen EJ, Beekman B, Te Koppele JM. Amino acid analysis by reverse-phase high-performance liquid chromatography: improved derivatization and detection conditions with 9-fluorenylmethyl chloroformate. Anal Biochem. 1996;240(2): 167-176.
- Saito M, Fujii K, Marumo K. Degree of mineralization-related collagen crosslinking in the femoral neck cancellous bone in cases of hip fracture and controls. Calcif Tissue Int. 2006;79(3):160-168.
- 74. Boyd RW. Nonlinear optics. 2003; pp 1-578.
- 75. Akin O, Göl K, Aktürk M, Erkaya S. Evaluation of bone turnover in postmenopausal patients with type 2 diabetes mellitus using biochemical markers and bone mineral density measurements. Gynecol Endocrinol. 2003;17(1):19-29.
- Sarkar PD, Choudhury AB. Relationship of serum osteocalcin levels with blood glucose, insulin resistance and lipid profile in central Indian men with type 2 diabetes. Arch Physiol Biochem. 2012; 118(5):260-264.
- 77. Sanchez-Enriquez S, Ballesteros-Gonzalez IT, Villafán-Bernal JR, et al. Serum levels of undercarboxylated osteocalcin are related to cardiovascular risk factors in patients with type 2 diabetes mellitus and healthy subjects. World J Diabetes. 2017;8(1):11-17.
- Zhou M, Ma X, Li H, et al. Serum osteocalcin concentrations in relation to glucose and lipid metabolism in Chinese individuals. Eur J Endocrinol. 2009;161(5):723-729.
- Riquelme-Gallego B, García-Molina L, Cano-Ibáñez N, et al. Circulating undercarboxylated osteocalcin as estimator of cardiovascular and type 2 diabetes risk in metabolic syndrome patients. Sci Rep. 2020;10(1):1-10.
- 80. Wang Q, Zhang B, Xu Y, Xu H, Zhang N. The relationship between serum osteocalcin concentration and glucose metabolism in patients with type 2 diabetes mellitus. Int J Endocrinol. 2013;2013: 842598.
- 81. Pittas AG, Harris SS, Eliades M, Stark P, Dawson-Hughes B. Association between serum osteocalcin and markers of metabolic phenotype. J Clin Endocrinol Metab. 2009;94(3):827-832.

- Saleem U, Mosley TH, Kullo IJ. Serum osteocalcin is associated with measures of insulin resistance, adipokine levels, and the presence of metabolic syndrome. Arterioscler Thromb Vasc Biol. 2010;30(7): 1474-1478.
- 83. Vaculík J, Braun M, Dungl P, Pavelka K, Stepan JJ. Serum and bone pentosidine in patients with low impact hip fractures and in patients with advanced osteoarthritis. BMC Musculoskelet Disord. 2016;17(1):308.
- 84. Tang SY, Zeenath U, Vashishth D. Effects of non-enzymatic glycation on cancellous bone fragility. Bone. 2007;40(4):1144-1151.
- 85. Torres AM, Matheny JB, Keaveny TM, Taylor D, Rimnac CM, Hernandez CJ. Material heterogeneity in cancellous bone promotes deformation recovery after mechanical failure. Proc Natl Acad Sci. 2016;113(11):2892-2897.
- 86. Semba RD, Fink JC, Sun K, Bandinelli S, Guralnik JM, Ferrucci L. Carboxymethyl-lysine, an advanced glycation end product, and decline of renal function in older community-dwelling adults. Eur J Nutr. 2009;48(1):38.
- 87. Nakano M, Nakamura Y, Suzuki T, et al. Pentosidine and carboxymethyl-lysine associate differently with prevalent osteoporotic vertebral fracture and various bone markers. Sci Rep. 2020; 10(1):1-11.
- 88. Arakawa S, Suzuki R, Kurosaka D, et al. Mass spectrometric quantitation of AGEs and enzymatic crosslinks in human cancellous bone. Sci Rep. 2020;10(1):18774.
- 89. Thomas CJ, Cleland TP, Sroga GE, Vashishth D. Accumulation of carboxymethyl-lysine (CML) in human cortical bone. Bone. 2018; 110:128-133.
- Raucci MG, Barboni B, Sprio S, et al. Mimicking the hierarchical organization of natural collagen: toward the development of ideal scaffolding material for tissue regeneration. Front Bioeng Biotechnol. 2021;9:644595.
- 91. Liu Y, Luo D, Wang T. Hierarchical structures of bone and bioinspired bone tissue engineering. Small. 2016;12(34):4611-4632.
- 92. Tehrani KF, Pendleton EG, Leitmann B, Barrow R, Mortensen LJ. Characterization of bone collagen organization defects in murine hypophosphatasia using a Zernike model of optical aberrations. SPIE. 2018;10497:162-168.
- Nadiarnykh O, Plotnikov S, Mohler WA, Kalajzic I, Redford-Badwal D, Campagnola PJ. Second harmonic generation imaging microscopy studies of osteogenesis imperfecta. J Biomed Opt. 2007;12(5): 051805.
- Edward Hoffler C, Edward Guo X, Zysset PK, Goldstein SA. An application of nanoindentation technique to measure bone tissue lamellae properties. J Biomech Eng. 2005;127(7):1046-1053.
- 95. Rho JY, Zioupos P, Currey JD, Pharr GM. Variations in the individual thick lamellar properties within osteons by nanoindentation. Bone. 1999;25(3):295-300.
- Mulder L, Koolstra JH, Den Toonder JMJ, Van Eijden TMGJ. Intratrabecular distribution of tissue stiffness and mineralization in developing trabecular bone. Bone. 2007;41(2):256-265.
- 97. Han ZH, Palnitkar S, Sudhaker Rao D, Nelson D, Parfitt AM. Effects of ethnicity and age or menopause on the remodeling and turnover of iliac bone: implications for mechanisms of bone loss. J Bone Miner Res. 1997;12(4):498-508.
- 98. Ott SM. Cortical or trabecular bone: what's the difference? Am J Nephrol. 2018;47(6):373-375.
- 99. Hein G, Weiss C, Lehmann G, Niwa T, Stein G, Franke S. Advanced glycation end product modification of bone proteins and bone remodelling: hypothesis and preliminary immunohistochemical findings. Ann Rheum Dis. 2006;65(1):101.
- Paschalis EP, Gamsjaeger S, Fratzl-Zelman N, et al. Evidence for a role for nanoporosity and pyridinoline content in human mild osteogenesis imperfecta. J Bone Mineral Res. 2016;31(5):1050-1059.
- Gamsjaeger S, Hofstetter B, Fratzl-Zelman N, et al. Pediatric reference Raman data for material characteristics of iliac trabecular bone. Bone. 2014;69:89-97.
- Heickendorff L, Ledet T, Rasmussen LM. Glycosaminoglycans in the human aorta in diabetes mellitus: a study of tunica media from

- areas with and without atherosclerotic plaque. Diabetologia. 1994; 37(3):286-292.
- Gowd V, Gurukar A, Chilkunda ND. Glycosaminoglycan remodeling during diabetes and the role of dietary factors in their modulation. World J Diabetes. 2016;7(4):67-73.
- Taylor EA, Donnelly E. Raman and Fourier transform infrared imaging for characterization of bone material properties. Bone. 2020; 139:115490.
- 105. Nyman JS, Makowski AJ, Patil CA, et al. Measuring differences in compositional properties of bone tissue by confocal raman spectroscopy. Calcif Tissue Int. 2011;89(2):111-122.
- 106. Currey JD. Role of collagen and other organics in the mechanical properties of bone. Osteoporos Int. 2003;14((Suppl 5)):S29-S36.
- Donnelly E, Chen DX, Boskey AL, Baker SP, Van Der Meulen MCH. Contribution of mineral to bone structural behavior and tissue mechanical properties. Calcif Tissue Int. 2010;87(5):450-460.
- Taylor EA, Lloyd AA, Salazar-Lara C, Donnelly E. Raman and Fourier transform infrared (FT-IR) mineral to matrix ratios correlate with physical chemical properties of model compounds and native bone tissue. Appl Spectrosc. 2017;71(10):2404-2410.
- Boskey A. Bone mineral crystal size. Osteoporos Int. 2003;14((Suppl 5)):16-21.
- 110. Jackuliak P, Kužma M, Payer J. Effect of antidiabetic treatment on bone [Internet]. Accessed 2022 Aug 20. Available from: www.biomed.cas.cz/physiolresPhysiol.Res.68
- 111. Gilbert MP, Pratley RE. The impact of diabetes and diabetes medications on bone health. Endocr Rev. 2015;36(2):194-213.

- 112. Thrailkill KM, Lumpkin CK, Bunn RC, Kemp SF, Fowlkes JL. Is insulin an anabolic agent in bone? Dissecting the diabetic bone for clues. Am J Physiol Endocrinol Metab. 2005;289(5):E735-E745.
- 113. Klein GL. Insulin and bone: recent developments. World J Diabetes. 2014;5(1):14.
- 114. Zhen D, Chen Y, Tang X. Metformin reverses the deleterious effects of high glucose on osteoblast function. J Diabetes Complications. 2010;24(5):334-344.
- 115. Mai QG, Zhang ZM, Xu S, et al. Metformin stimulates osteoprotegerin and reduces RANKL expression in osteoblasts and ovariectomized rats. J Cell Biochem. 2011;112(10):2902-2909.
- 116. Zinman B, Haffner SM, Herman WH, et al. Effect of rosiglitazone, metformin, and glyburide on bone biomarkers in patients with type 2 diabetes. J Clin Endocrinol Metab. 2010;95(1):134-142.
- 117. Poundarik AA, Wu PC, Evis Z, et al. A direct role of collagen glycation in bone fracture. J Mech Behav Biomed Mater. 2015;50:82-92.
- 118. Willett TL, Sutty S, Gaspar A, Avery N, Grynpas M. In vitro nonenzymatic ribation reduces post-yield strain accommodation in cortical bone. Bone. 2013;52(2):611-622.
- 119. Tang SY, Vashishth D. The relative contributions of non-enzymatic glycation and cortical porosity on the fracture toughness of aging bone. J Biomech. 2011;44(2):330.
- 120. Acevedo C, Sylvia M, Schaible E, et al. Contributions of material properties and structure to increased bone fragility for a given bone mass in the UCD-T2DM rat model of type 2 diabetes. J Bone Miner Res. 2018;33(6):1066-1075.